Lipid Rafts Prepared by Different Methods Contain Different Connexin Channels, but Gap Junctions Are Not Lipid Rafts†

Darren Locke,* Jade Liu, and Andrew L. Harris

Department of Pharmacology and Physiology, MSB I-645, New Jersey Medical School, University of Medicine and Dentistry of New Jersey, 185 South Orange Avenue, Newark, New Jersey 07103

Received March 17, 2005; Revised Manuscript Received July 27, 2005

ABSTRACT: Cell extraction with cold nonionic detergents or alkaline carbonate prepares an insoluble membrane fraction whose buoyant density permits its flotation in discontinuous sucrose gradients. These lipid "rafts" are implicated in protein sorting and are attractive candidates as platforms that coordinate signal transduction pathways with intracellular substrates. Gap junctions form a direct molecular signaling pathway by end-to-end apposition of hemichannels containing one (homomeric) or more (heteromeric) connexin isoforms. Residency of channels composed of Cx26 and/or Cx32 in lipid rafts was assessed by membrane insolubility in alkaline carbonate or different concentrations of Triton X100, Nonidet P40 and Brij-58 nonionic detergents. Using Triton X100, insoluble raft membranes contained homomeric Cx32 channels, but Cx26-containing channels only when low detergent concentrations were used. Results were similar using Nonidet P40, except that Cx26-containing channels were excluded from raft membranes at all detergent concentrations. In contrast, homomeric Cx26 channels were enriched within Brij-58-insoluble rafts, whereas Cx32-containing channels partitioned between raft and nonraft membranes. Immunofluorescence microscopy showed prominent colocalization only of nonjunctional connexin channels with raft plasma membrane; junctional plaques were not lipid rafts. Rafts prepared by different extraction methods had considerable quantitative and qualitative differences in their lipid compositions. That functionally different nonjunctional connexin channels partition among rafts with distinct lipid compositions suggests that unpaired Cx26 and/or Cx32 channels exist in membrane domains of slightly different physicochemical character. Rafts may be involved in trafficking of plasma membrane connexin channels to gap junctions.

The Singer−Nicholson fluid mosaic model proposed that the plasma membrane is a neutral two-dimensional "solvent" for membrane proteins (*1*). However, biophysical and biochemical study of "model" lipid bilayers show that interspersed plasma membrane lipids will segregate into gel-like liquid-ordered (*l*o or *lβ*)[1] and/or fluid liquid-disordered (*l*d or *lα*) phases (*2*, *3*). In the former state, phospholipids with long saturated acyl chains intercalate with cholesterol, this conferring a structural rigidity that limits the lateral mobility of *l*o lipid patches in the surrounding, supportive *l*d phospholipid milieu. This has been confirmed, still somewhat controversially, in the exoplasmic membrane leaflet where these cohesive lipid patches are enriched in sphingolipids and cholesterol while remaining segregated from bulk membrane glycerolipids (*4*). Such microdomains, known commonly as lipid "rafts", are resistant to solubilization by cold nonionic detergents or to cold sodium carbonate extraction at high alkaline pH (*5*−*7*). Their buoyant density, due to their higher lipid/protein ratio compared with bulk membrane, permits their flotation in and recovery from discontinuous sucrose gradients after isopycnic centrifugation.

The concept of the lipid raft has proliferated into many cellular systems (*4*). Rafts have been implicated in efficient and specific intracellular signaling interactions (*5*, *8*). Since rafts also selectively include and exclude specific proteins, rafts may also have functional relevance with respect to protein sorting (*9*). Members of all families of membrane channels have been found within rafts (*10*, *11*). Since channels are important initiators of many signal transduction pathways, raft localization may ensure their proximity to signaling modulators, permitting dynamic regulation of channel function(s) and vice versa.

Membrane channels composed of connexin proteins occupy a specialized niche. Gap junction plaques, which are large discrete and ordered accretions of connexin channels, provide a direct and focused intercellular signaling pathway between juxtaposed cells. Intercellular channels form by end-to-end apposition of single-membrane hemichannels composed of one (homomeric) or more (heteromeric) members of the connexin superfamily, of which there are ∼20 members. These channels facilitate the sharing of cytoplasmic ions and molecules by coupled cells, which appears to be essential for normal cellular development and function (*12*).

† Supported by NIH Grants GM36044 and GM61406 to A.L.H.

* Corresponding author. Tel: 001 973 972 1619. Fax: 001 973 972 4554. E-mail: lockeda@umdnj.edu.

[1] Abbreviations: CA, cardiolipin; Chol, cholesterol; CTB-FITC, cholera toxin B subunit labeled with fluorescein isothiocyanate; CTB-HRP, cholera toxin B subunit labeled with horseradish peroxidase; CMTX, Charcot-Marie tooth disease, X-linked; CT, carboxyl-tail; Cx26, connexin26; Cx32, connexin32; FAME, fatty acid methyl ester; FID, flame ionization detection; GC, gas chromatography; GM_1, ganglioside GM_1; HA, hemagglutinin; HLB, hydrophile−lipophile balance; $(HN)_6$, six repeats of His-Asn; NP-HPLC, normal phase high pressure liquid chromatography; l*d*, liquid-disordered membrane; l*o*, liquid-ordered membrane; LPE, lysophosphatidylethanolamine; NP40, Nonidet P40; PC, phosphatidylcholine; PG, phosphatidylglycerol; TG, triglyceride; TM1, the first connexin transmembrane domain; TX100, Triton X100.

10.1021/bi050495a CCC: $30.25
Published on Web 09/08/2005

In addition to regulatory differences (reviewed in ref *13*), dramatic and surprising degrees of ionic and molecular selectivity of permeation through connexin channels, and differences in this selectivity, have been observed solely as functions of the connexin composition (*14*−*18*).

Gap junctions between hepatocytes (Cx26 and/or Cx32 channels) (*19*) and lens fiber cells (Cx46 and/or Cx50 channels) (*20*) are enriched in cholesterol and sphingomyelin, a saturated acyl-chain phospholipid. Such lipids suggest a high structural membrane rigidity of the gap junction plaque, akin to *l*o raft microdomains of membranes. These lipid environments may exert significant constraints on the lateral movements of accreted connexin channels, and perhaps the membrane localizations and/or movements of unpaired hemichannels. Recent evidence linking connexin channels with raft domains is the association of some connexin proteins with the monotopic cholesterol-binding protein caveolin-1 (*21*, *22*), one of the structural membrane proteins of caveolae. Caveolae are one subpopulation of lipid rafts; their lipid profile and biochemical properties clearly designate them as rafts, whereas the invaginated morphology and the scaffolding protein caveolin set them apart from other raft types (*23*).

It has recently become clear that different extraction/enrichment procedures may isolate different subsets of lipid rafts (*2*, *3*, *5*−*8*, *24*−*26*). To date, there has not been a systematic study of the distribution of a specific class of membrane channel among raft subsets obtained by different isolation procedures. In this study, we examined the localization of homomeric and heteromeric Cx26 and/or Cx32 channels to raft membranes prepared by different methods. Whereas gap junctions did not appear to be lipid raft membranes, nonjunctional channels formed by Cx26 or Cx32, or both Cx26 and Cx32, were raft associated. Nonionic detergents revealed the differential distribution of Cx26 and/or Cx32 channels among rafts, yet, when prepared by detergent-free alkaline carbonate extraction (known to enrich caveolae), all channels were raft-associated. As such, gap junctions must share much of the established biochemical and physicochemical character of lipid raft domains, yet cannot be considered as rafts. Rafts prepared by different methods showed considerable quantitative and qualitative differences in their lipid content(s). Such differential protein−lipid associations are likely to have important functional consequences for trafficking of connexin channels and intercellular signaling through gap junctions.

MATERIALS AND METHODS

All components for the HeLa-connexin expression system (*27*) were from BD Biosciences (Palo Alto, CA). DMEM, G418, doxycycline, and hygromycin were from Life Technologies (Rockville, MD). Monoclonal anti-caveolin-1 antibody and monoclonal anti-Cx26 antibody were from Zymed (San Francisco, CA). Monoclonal anti-CD71 was from Santa Cruz Biotechnologies (Santa Cruz, CA). Cx32 was detected using monoclonal M12.13 anti-Cx32 mouse antibody (*17*). Anti-HA clone HA-7 mouse IgG was from Sigma (St. Louis, MO). All other reagents were from Sigma, unless stated otherwise.

Functional Expression of HA(HN)$_6$-Tagged Connexin Hemichannels in HeLa Cells. Bidirectional tetracycline (Tet)-responsive expression vectors (pBI; Clontech, San Diego, CA), containing one or two available multiple cloning sites, were used to express homomeric or heteromeric connexin channels, respectively, in "TetOn"-HeLa cells (*27*). HeLa cells were used due to their virtual lack of endogenous connexin expression. Connexins were subcloned into one of the available cloning sites, in frame with a carboxyl-terminal (CT) 3.3 kDa "tag" that includes a thrombin cleavage site preceding a hemagglutinin (HA) and 6xHis-Asn epitope (HA(HN)$_6$). When both cloning sites contained connexin sequences for coexpression, only one of the two connexins (as heteromeric channels) was tagged.

HeLa cells (homomeric lines Cx26Tag or Cx32Tag, and heteromeric lines Cx26Tag/Cx32 or Cx26/Cx32Tag) were maintained in 200 mg/mL hygromycin B and 100 mg/mL G418. Connexin expression was induced with 1 mg/mL doxycycline for 48 h. Connexin localized to HeLa plasma membranes, shown by immunofluorescence, forming intercellular gap junctions permeable to Lucifer yellow (scrape-loading; data not shown) or calcein, reliable indicators of pore function (Figure 1). Calcein dye permeability was assessed using a donor-receiver junctional coupling assay. In brief, dye donor and dye receiver cells were induced for connexin expression. At 48 h post-Tet-induction, donor cells were labeled with the membrane dye CM-DiL (5 μM; Molecular Probes, Eugene, OR) and the gap junction permeant dye calcein-AM (5 μM; Molecular Probes) for 30 min. After washing, donor cells were seeded onto nonconfluent receiver cells and allowed to attach for 3 h, and then monolayers were evaluated for calcein transfer from donor (marked by CM-DiL) to receiver (calcein only) cells. When immunoaffinity purified using the HA(HN)$_6$ tag, and reconstituted into unilamellar liposomes, connexin from all cell lines shows channel activity ex vitro by Transport Specific Fractionation analysis (*27*).

Purification of Detergent-Insoluble Lipid Rafts Using Discontinuous Sucrose Gradients. Lipid rafts were prepared from 48 h post-Tet-induced HeLa cell lines grown to confluence in 100 mm^2 dishes. All solutions, materials, and handling were at 0−4 °C. After three washes with raft buffer (50 mM MES, 100 mM NaCl pH 6.5), cells were scraped into raft buffer containing protease inhibitors and SurfactAmps grade Brij-58, Nonidet P40 (NP40) or Triton X100 (TX100) (Pierce-Endogen, Rockford, IL). Detergent was added to raft buffer from 10% w/v stock solutions to percentage w/v concentrations indicated in the text or figures. As NP40 and TX100 are subject to autoxidation, to avoid impurities that would affect the cell extractions, all stock detergent solutions (including Brij-58) were sealed under nitrogen, kept out of direct light, in glass vials that were discarded once opened. Homogenization was carried out using a loose-fitting Dounce and by passing the homogenate through a 25G needle. The homogenate was adjusted to ∼40% w/v sucrose by addition of 2 volumes of 63% w/v sucrose prepared in raft buffer that contained the same percentage w/v concentration of detergent as lysis buffer. A discontinuous gradient was formed above the lysate (2 mL of 30% w/v sucrose and 10% w/v sucrose, to fill tube, in raft buffer with neither step containing detergent). Gradients were centrifuged at 4 °C for 18 h at 44 000 rpm (200000g_{av}) using a Beckman SW60Ti rotor. Twelve fractions were collected at 0−4 °C using a 100 μL capillary pipet from top to bottom; fraction twelve typically contained the detergent-

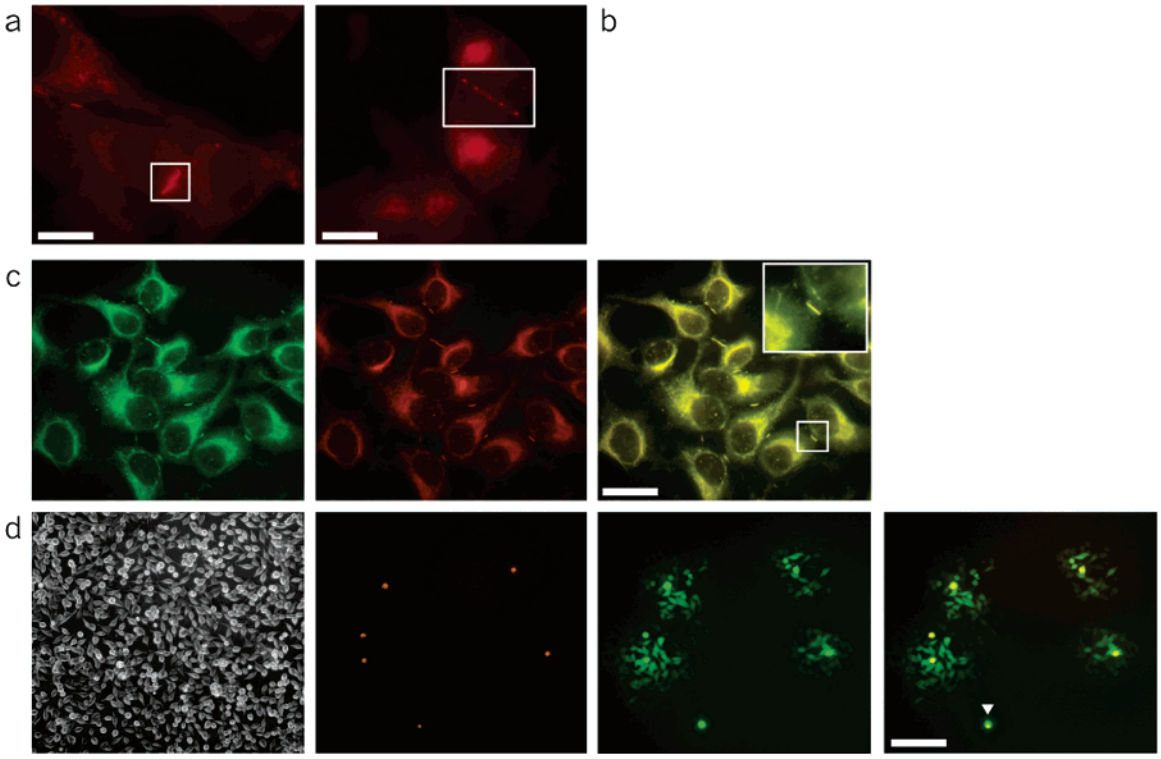

FIGURE 1: Stable gap junction-expressing HeLa cell lines. HeLa-"TetOn" cells were transfected with tetracycline-responsive pBI vectors coding for rCx26 or rCx32, or both rCx26 and rCx32. Connexins were tagged at their CT with a $HA(HN)_6$ tag. Immunofluorescence localization of homomeric Cx26 (a) and Cx32 (b) channels in HeLa cell lines is shown using mouse anti-HA and Alexa594-conjugated secondary, following 48 h induction with doxycycline. Punctate staining at regions of cell−cell contact is indicative of gap junction formation (boxed). In heteromeric channels either Cx26 or Cx32 was CT tagged, but not both. Colocalization of Cx26Tag and Cx32 in the same gap junctions (48 h induction with doxycycline) is shown using rabbit anti-Cx26 with FITC labeled secondary (green), and mouse anti-Cx32 M12.13 with Alexa594 labeled secondary (red). Staining at junctional membrane is superimposable (c; yellow, boxed, higher magnification of junction shown inset). Bar 5 μm. Dye transfer in stable connexin-transfected cell lines (d) shows junctional transfer of calcein (green) from calcein-AM/CM-DiL (red-orange) labeled donor cells to unlabeled receiver cells. Bar 50 μm.

soluble cell pellet (*28*). The sucrose concentration of each fraction was determined using an ATC refractometer (Sun Instruments, Torrance, CA) with temperature correction. Density was calculated using interactive tables at www.univ-reims.fr/Externes/AVH/MementoSugar/001.htm.

Detergent-Free Purification of Lipid Rafts. HeLa cell lines (48 h post-Tet-induction), grown to confluence in 100 mm^2 dishes, were used to prepare lipid rafts at 0−4 °C using 0.5 M Na_2CO_3 pH 11 (*29*). After homogenization, the samples were sonicated at low power (3 × 20 s bursts). Centrifugation time, speed, and fraction recovery were as per isolation of detergent-insoluble rafts.

Protein Quantification of Gradient Fractions. The profile of protein concentration in the discontinuous sucrose gradients was determined by Micro-BCA assay kit (Pierce-Endogen) on 50 μL fraction aliquots (volume adjusted) using supplied BSA as standard.

Protein Recovery from Gradient Fractions. All protein in each gradient fraction was used for Western blotting. To each, 2 volumes of cold MeOH was added, the sample vortexed, and 1 volume of cold $CHCl_3$ added. For phase separation, 1.5 volumes of cold water was added, and the samples were vortexed and centrifuged at $10000g_{av}$ (5 min). The upper phase was discarded, and 1.5 volumes of cold MeOH was added to the lower phase and protein interface. The samples were mixed and centrifuged ($14000g_{av}$, 5 min) to pellet the protein. Pellets were dissolved in 2 × Laemmli SDS−PAGE sample buffer.

Recovery of Total Lipid from Gradient Fractions. Lipids were extracted from gradient fractions by an acid Bligh−Dyer method (*30*) using MeOH and $CHCl_3$-washed glassware. Briefly, samples were vortexed with 3.75 volumes of 50:100:1.5 v/v $CHCl_3$:MeOH:HCl, and then 1.25 volumes of $CHCl_3$ (vortex) and 1.25 volumes of filtered double distilled water (vortex) were added. Samples were left to stand for ∼10 min and then centrifuged at $1000g_{av}$ for 5 min at rt. The lower phase was recovered to a cleaned glass tube using a cleaned glass Pasteur pipet by applying positive pressure through the upper phase to avoid contaminating the samples. To avoid contamination, not all of this lower phase was recovered. Extracted lipids were dried under argon, subsequently in a vacuum desiccator for ∼30 min, and then stored at −70 °C.

Cholesterol Assay of Gradient Fractions. To dried lipid samples of gradient fractions and a set of cholesterol standards, 0.75 mL of acetic acid and 0.50 mL of ferric chloride reagent were added. Ferric chloride reagent was prepared by diluting 2.5% w/v $FeCl_3$ in 85% w/v H_3PO_4 (total volume 2 mL) to 25 mL with concentrated H_2SO_4. A purple color developed after ∼15 min, and absorbance at 550 nm was recorded (*31*).

Cholesterol Depletion from HeLa Cells. To remove cholesterol from the plasma membrane of post-Tet-induced HeLa cell lines, confluent 100 mm^2 dishes were washed twice with 0.1 M PBS pH 7.4 and incubated with 10 mM methyl β-cyclodextrin (*32*) or the inactive control, 10 mM α-cy-

clodextrin, in 0.1 M PBS pH 7.4 for 1 h at 37 °C. Cells were washed twice in ice-cold 0.1 M PBS pH 7.4 to remove free cyclodextrin and methyl β-cyclodextrin:cholesterol complexes prior to raft isolation.

Phospholipid Analysis of Gradient Fractions. For the measurement of phosphates, dried lipids were resolubilized in 50 μL of 1% w/v SDS at 37 °C, and then 0.40 mL H_2SO_4 was added. The tubes were heated to ~200 °C for 30 min and allowed to cool, and then 150 μL H_2O_2 was added. Heating was continued for an additional 30 min. Once cooled, 3.9 mL of deionized water was added to all tubes. The final solution was mixed with 0.125 volume of 2.5% w/v ammonium molybdate in 2.5 M sulfuric acid and 0.050 volume of fresh, filtered Fiske−Subbarow reagent (0.5 g of amino-naphthol-sulfonic acid in 200 mL of 15% anhydrous $NaHSO_4$ containing 1 g of anhydrous Na_2SO_3). After incubation for 30 min at rt, the absorbance was measured at 600 nm alongside a H_2PO_4 standard curve (*33*).

GM_1 Ganglioside Analysis of Gradient Fractions. Lipid raft GM_1 ganglioside in raft fractions was detected using the B subunit of cholera toxin (CTB) conjugated to peroxidase (HRP) (CTB-HRP; Calbiochem, La Jolla, CA). First, 2.5 μL aliquots (equivalent volumes) of each gradient fraction were spotted (~5 mm ∅) onto dry nitrocellulose. After all spots had dried, membranes were blocked in 0.1 M PBS pH 7.4 and 1% w/v BSA, and then probed with CTB-HRP (1/10 000 dilution of 2 purpurogallin units/mL stock) in 0.1 M PBS pH 7.4 and 1% w/v BSA. After washing, specific interactions were shown using an HRP-conjugate substrate kit (Biorad, Hercules, CA) (*28*). The second method involved prelabeling 100 mm^2 confluent dishes of 48 h post-Tet-induced HeLa cell lines with CTB-HRP (1/5000 dilution stock in 0.1 M PBS pH 7.4) for 30 min at 0−4 °C (*34*). Cells were washed twice in ice-cold 0.1 M PBS pH 7.4, which removes unbound CTB-HRP, and lipid rafts were prepared as described. After collection of gradient fractions, 25 μL aliquots of each fraction (equivalent volumes) were assayed (along with CTB-HRP standards, i.e., dilution of stock CTB-HRP) using a chromogenic peroxidase substrate, ABTS (in ABTS buffer; Roche, Indianapolis, IN). A dark-green color was allowed to develop at 37 °C, and absorbance was read at 405 nm.

Cell Surface Labeling of GM_1 Ganglioside and Immunofluorescence Microscopy. To label cell surface GM_1 ganglioside for microscopy, HeLa cells grown on 12 mm ∅ glass coverslips were incubated for 30 min at 4 °C with 10 μg/mL CTB coupled to FITC (CTB-FITC), prepared in bicarbonate-free DMEM and 0.5% BSA (*35*). The cells were washed five times, and fixed with 4% w/v paraformaldehyde for 10 min (dark), washed extensively, then lightly permeabilized for 2 min with 0.1% w/v TX100 at 0−4 °C (dark). Cells were labeled post-fix for Cx26 and/or Cx32 with the appropriate primary antibodies diluted in 0.1 M PBS pH 7.4, 1% w/v BSA and visualized using Alexa594-conjugated secondary antibodies (Molecular Probes), as indicated. Cells were also labeled with CTB-FITC for 30 min at 37 °C, which leads to rapid internalization of CTB-FITC labeled membrane to Golgi and/or endosomes via a caveolae/raft-dependent pathway (*35*). Fluorescently labeled cells were visualized with the 100× planapochromat oil objective of a Zeiss Axiovert 100 microscope.

Isolation and Solubility of HeLa Cell Plasma Membranes. Plasma membranes were prepared from 48 h post-Tet-induced HeLa cell lines grown to confluence in 500 mm^2 dishes. All solutions, materials, and handling were at 0−4 °C. After washes in 0.1 M PBS pH 7.4, cells were scraped into 10 mM HEPES, 1 mM EDTA pH 7.4 containing 8.7% w/v sucrose and protease inhibitors (HEPES-sucrose buffer). Cells were collected by centrifugation at 4 °C for 15 min at 7500 rpm ($4400g_{av}$) using a Beckman Ti45 rotor. The cell pellet was resuspended in HEPES-sucrose buffer and sonicated for 3 × 10 s at low power. The sonicate was layered onto a step gradient of 1.0 mL of 50% w/v sucrose (bottom step) and 2.0 mL of 27% w/v sucrose, both in HEPES-sucrose buffer. Gradients were centrifuged at 4 °C for 2 h at 45 000 rpm ($208000g_{av}$) using a Beckman SW60Ti rotor, and plasma membranes recovered from the 27:50% w/v sucrose interface (*36*). Membranes were washed twice in 10 mM HEPES, 5 mM EDTA pH 7.4 by centrifugation at 4 °C for 30 min at 30 000 rpm ($92000g_{av}$) using a Beckman SW60Ti rotor, and resuspended in 1 mL of raft buffer (50 mM MES, 100 mM NaCl pH 6.5) containing detergent. Harvested membranes were "solubilized" for 20 min at 0−4 °C by Brij-58 or Triton X100 (TX100) at percentage w/v concentrations indicated in the text or figures. Detergent-soluble and detergent-insoluble (pellet) fractions were isolated by centrifugation at 4 °C for 30 min at 40 000 rpm ($100000g_{av}$) using a Beckman TLA45 rotor. SDS was added to the pellet and supernatant at 1% w/v and final volume 500 μL.

Separation of Phospholipids by HPLC. Dried lipid was dissolved in 1:1 v/v $CHCl_3$:MeOH at a concentration of 2 mg/mL. Sample (200 μL into a 20 μL loop) was loaded onto an Astec 5 mm diol-bonded silica normal phase spherical column (250 × 4.6 mm; Advanced Separation Technology, Whippany, NJ). The column was eluted at 1.25 mL/min at 40 °C using mobile phase A (60:39:1 v/v/v $CHCl_3$:MeOH:NH_4OH) and B (60:34:5:1 v/v/v/v $CHCl_3$:MeOH:H_2O:NH_4-OH). The following program was run: From 0 to 14 min linear gradient 100% A to 100% B, 14−25 min hold 100% B, 25−30 min linear gradient 100% B to 100% A, 30−45 min hold 100% A to regenerate. Standards were a 1 mg/mL mix of triolein, cholesterol, ceramide, oleic acid, 18:1 phosphatidylcholine, 18:1 phosphatidylglycerol, 18:1 phosphatidylethanolamine, 18:1 phosphatidylserine, 18:1 phosphatidic acid, soy phosphatidylinositol, sphingomyelin, and a 0.5 mg/mL mix of 18:1 lysophosphatidylcholine, 18:1 lysophosphatidylethanolamine, 18:1 lysophosphatidylglycerol, 18:1 lysophosphatidylserine, and 14:0 cardiolipin (all Avanti Polar Lipids, Alabaster, IL). The eluate was analyzed by evaporative light scattering using a Sedex 55 ELSD, and a five level calibration curve was used to calculate the amount of lipid species in each sample.

Fatty Acid Analysis of Phospholipids Using GC. Fatty acids undergo methylation of the carboxylic acid function to form fatty acid methyl esters (FAMEs). FAMEs were identified and quantitated using a Hewlett-Packard 5890 series II gas chromatograph coupled with a J & W fused silica capillary column DB-225 (30M × 0.2 mm, 0.25 μm film; Agilent, Wilmington DE) and flame ionization detection unit (FID). Column temperature was 220 °C, injector temperature was 250 °C, and 15 psi of nitrogen was used as carrier gas. Column flow was 1 mL/min (split flow 20:1) with run time 25 min. Reference standard No. 68A (Nu-Chek-Prep Inc, Elysian, MN) was used for FAMEs of C_4 to

C_{24} fatty acids. Dried sample lipids were diluted with toluene (0.2 mL) and 1% v/v H_2SO_4 in CH_3OH (0.4 mL), and then heated at 70 °C for 30 min. This methylated both esterified and free fatty acids. Methylated samples were cooled, 1.0 mL of hexane and 1.0 mL of water were added, and then the samples were centrifuged. The upper hexane phase containing FAMEs was collected and dried under nitrogen. FAMEs were reconstituted in hexane to an appropriate concentration. To 1 mL of sample in hexane was added 50 μL of 1 N CH_3ONa, and, after 5 min at rt, the sample was centrifuged at $1600g_{av}$ for 5 min. The FAME standard was run in the first available position, a NIH-Reference standard F (Alltech, Deersfield, IL) in the second position, and a hexane solvent blank in the third position. The concentrations of standards were determined by gravimetric analysis at 20 mg/mL. The sample was in the fourth position. The limit of detection was 0.03% w/w of the original sample. The limit of quantitation for the method is 0.1% w/w original sample. No impurity or fraction was reported that was less than 0.1% w/w.

RESULTS

Even though the lipid composition of membrane rafts is well defined by their dependence on cholesterol and saturated phospholipids (*1*, *4*), there is no generally agreed isolation scheme. Two methods are commonly used to isolate rafts and rely on their resistance to solubilization by high pH alkaline carbonate or by nonionic detergents, both at 0−4 °C (*5*−*7*). The low temperature is necessary as rafts are increasingly soluble at higher temperatures. Insoluble rafts are typically enriched and separated from other insoluble membranes by isopycnic density gradient centrifugation. However, current thought is that different extraction methods for isolating raft membranes may define different subsets of membrane rafts (*2*, *3*, *5*−*8*, *24*−*26*).

Establishment of Stable HeLa Cells Lines That Inducibly Express Homomeric Cx26, Homomeric Cx32, or Heteromeric Cx26/Cx32 Channels. We recently described a strategy for the expression of recombinant homomeric and heteromeric connexin channels in communication-incompetent HeLa cells, mimicking in vivo channel compositions (see Materials and Methods, ref *27*, and Figure 1). Tetracycline-responsive vectors allowed the inducible expression of different Cx26 and/or Cx32 channels in which the connexins are $HA(HN)_6$ tagged; in heteromeric channels either Cx26 or Cx32 is tagged, but not both. The natural heterogeneity of Cx26 and Cx32 is such that, when both connexins are expressed together, heteromeric pores are the dominant channel form (*27*, *37*). These homomeric and heteromeric Cx26 and/or Cx32 channels have connexin-specific differences in the size selectivity of their permeability pathways, in molecular selectivity, among second messengers, and modulation by cellular factors (*14*, *17*).

This expression system was used to determine the distribution of homomeric and heteromeric Cx26 and/or Cx32 connexin channels among raft domains of HeLa cells. Rafts were prepared by established protocols, by a detergent-free method or using three nonionic detergents (see Materials and Methods). Connexin was identified by monoclonal antibodies specific to Cx26 and/or Cx32, and/or the CT $\underline{HA}(HN)_6$ tag. For these studies, the ganglioside GM_1, a glycerophospholipid in the outer layer of the membrane leaflet, was used as the raft marker (*34*). GM_1 is a high-affinity binding site for the B subunit of cholera toxin (CTB), which was covalently linked to a peroxidase (HRP) or fluorescein (FITC) reporter. The membrane protein CD71 (transferrin receptor) is known to be completely solubilized by cold detergent (*26*, *38*) and was used as a protein marker for nonraft fractions.

Alkaline Sodium Carbonate Extraction of HeLa Membranes: Connexin-Enriched Raft Fractions. Detergent-free extraction (0.5 M Na_2CO_3 pH 11) is typically used to prepare caveolar raft membranes, specialized raftlike invaginations of cell membrane (*23*, *29*). Connexin proteins may interact with the monotopic cholesterol-binding protein caveolin-1 (*21*, *22*), a structural membrane protein of caveolae (*23*). Homomeric Cx26 and homomeric Cx32 channels were found in light density alkaline carbonate insoluble fractions (Figure 2a), which were enriched for caveolin-1 and GM_1 ganglioside marker (raft), as shown by dot blot of the gradient fractions with CTB-HRP. Heteromeric Cx26/Cx32 channels showed some partitioning between carbonate-insoluble raft and nonraft gradient fractions whereas the homomeric channels did not. CD71 was always found within the nonraft sucrose gradient fractions. Caveolin-1 has a consensus binding sequence ΦXΦXXXXΦ in the first transmembrane domain, TM1, of many connexins (Figure 2b; Φ, aromatic amino acid; *39*), and physical interactions between caveolin-1 and Cx26 or Cx32 have been reported in Triton X100 insoluble membranes of HEK293T cells (*22*).

Cholesterol Depletion Leads to "Solubilization" of Connexin-Containing Raft Fractions Isolated by Alkaline Sodium Carbonate Extraction. Cohesive forces between cholesterol and saturated hydrocarbon chains stabilize the raft phase in the phospholipid milieu of the plasma membrane (*2*−*5*). For this reason, cholesterol-depleting agents will disrupt lipid rafts (*32*, *40*). Cholesterol depletion by methyl β-cyclodextrin, but not α-cyclodextrin (data not shown), led to dissolutions of raft microdomains (*40*) and therefore changed the flotation position of caveolin-1 membranes (a cholesterol-binding protein). The flotation profiles of homomeric (Figure 2c) and heteromeric (data not shown) connexin channels were also altered by methyl β-cyclodextrin treatment, whereas flotation profiles of CD71 remained unchanged. These data show a correlation between integrity of cholesterol-based raft membranes and connexin localization, when alkaline carbonate is used for raft preparation.

Extraction of HeLa Cells with Different Nonionic Detergents Prepares Raft Fractions That Contain Different Connexin Channels. Classically, TX100 (at 1.00% w/v) is used to prepare raft membranes. However, previous studies on the association or recruitment of membrane proteins to rafts have used detergents other than TX100, or TX100 concentrations lower than 1% w/v (*28*, *38*, *41*). Brij-58, Nonidet P40 (NP40), and Triton X100 (TX100) were used for raft extraction from HeLa membranes (Table 1); a short summary of their physicochemical differences and similarities is found in the table footnote. Each detergent has been used previously to prepare lipid rafts from a variety of cell types, including HeLa cells (*5*, *9*). We sought to identify if connexin channels were present in detergent-insoluble rafts, and whether different detergents were capable of isolating raft subsets, also containing different connexin channels.

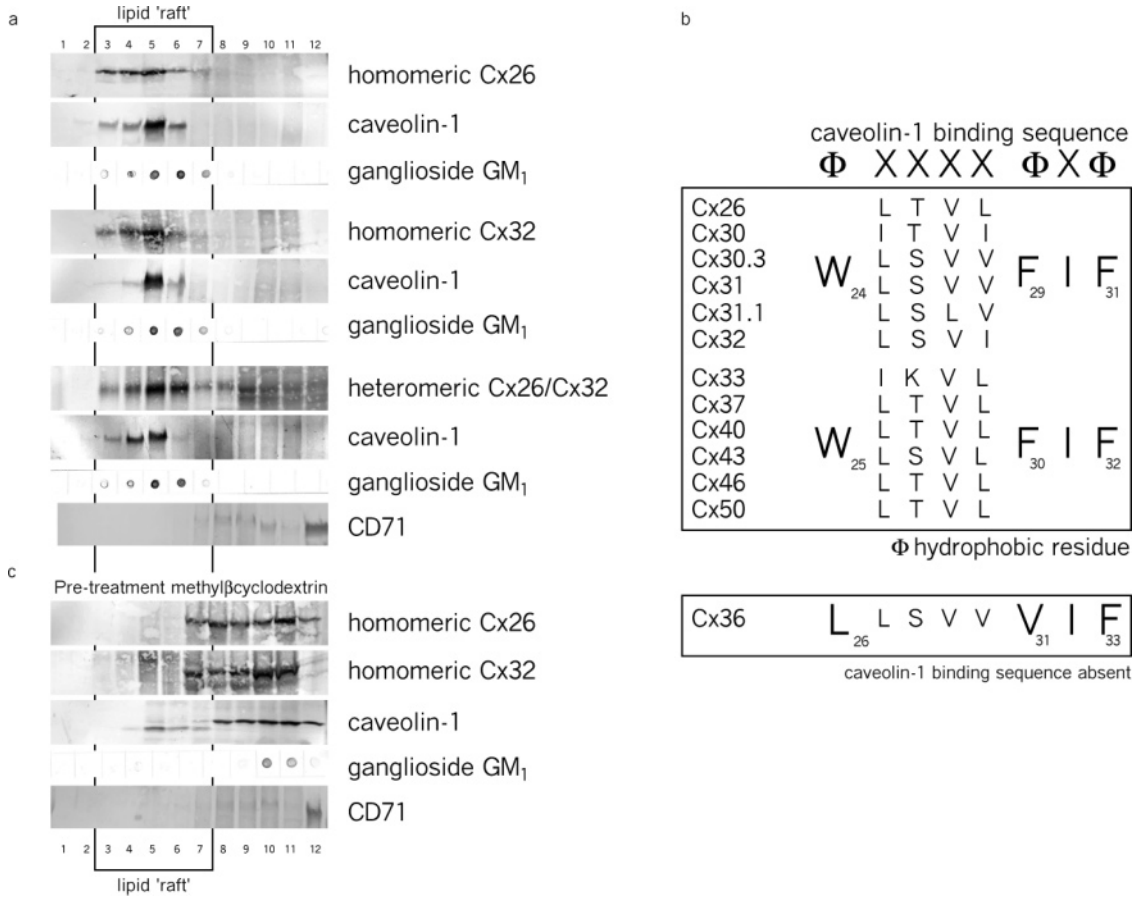

FIGURE 2: Cx26 and/or Cx32 channels are associated with lipid raft fractions prepared by alkaline carbonate extraction. (a) Raft fractions prepared by 0.5 M Na_2CO_3 pH 11 extraction of HeLa cells enrich caveolin-1, and all connexin channels studied. Data shown is representative of three independent experiments. The ganglioside GM_1 is used as the raft marker. Dot blots beneath each Western blot represent the binding of pentavalent CTB-HRP to an aliquot of the respective gradient fraction from which the protein was then recovered. Western blotting was with monoclonal anti-HA to the CT $HA(HN)_6$ "tag" and/or monoclonal antibodies specific to Cx26 or Cx32 when heteromeric channels were expressed (only one connexin in these channels is CT tagged). Heteromeric channels shown in the figure are Cx26Tag/Cx32, and all blots shown are with anti-HA for comparative purposes. Rafts are largely within fractions 5 and 6 of 12 collected fractions, fraction 1 being the first collected and lightest, and fraction 12 the heaviest. The membrane protein CD71, a nonraft protein, was found in the heavier sucrose gradient fractions and not in fractions that contained GM_1. (b) A conspicuous caveolin-1 binding sequence is found in TM1 of all rat connexin isoforms except rCx36. (c) As caveolin-1 is a cholesterol-binding protein, depletion of cholesterol from the outer leaflet of the plasma membrane with methyl β-cyclodextrin led to changes in the flotation of caveolin-1, homomeric Cx26 and/or Cx32 homomeric channels (heteromeric data not shown here) and dissolution of raft. The flotation profile of CD71 remained unchanged.

Table 1: Physicochemical Properties of Detergents Used for Raft Preparation[a]

Detergent	CMC mM	CMC % w/v	HLB	Structure	Other
Brij-58	0.077	0.0086	15.7	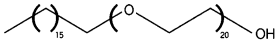	1123.52 Da
Nonidet P40	0.29	0.058	13.1	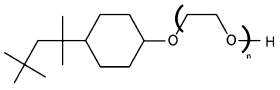	602 Da, n = 9.0 (chain length ~14 Å)
Triton X100	0.24	0.151	13.5		647 Da, n ≅ 10.0, (chain length ~15-16 Å)

[a] The nonionic detergents Brij-58, Nonidet P40 (NP40), and Triton X100 (TX100) were used to prepare lipid rafts using discontinuous sucrose gradients (*61*). The Brij family are polyoxyethylene fatty ethers derived from lauryl, cetyl, stearyl, and oleyl alcohols. Brij-58 is the C_{20} polyoxyethylene cetyl ether with an unsaturated $C_{16:0}$ chain. NP40 and TX100 are members of the octylphenol ethoxylate family. They differ in the length of the hydrophilic oxyethelene group. The lower hydrophile−lipophile balance (HLB; an index of detergent hydrophilicity) of the shorter chain NP40 means that it is slightly more hydrophobic than TX100. Brij-58 molecule is more hydrophilic; the HLB of Brij-58 is greater than that of TX100 or NP40. The critical micelle concentration (CMC) is the concentration above which detergent micelles form.

Figure 3 shows the sucrose gradient distribution of homomeric Cx26, heteromeric Cx26/Cx32, or homomeric Cx32 channel types after isopycnic centrifugation of HeLa cells that were solubilized in 0.25−2.00% w/v TX100. Lipid raft fractions from cell lines expressing heteromeric channels (with the CT $HA(HN)_6$ "tag" on either connexin) were identical by Western blot in their connexin localizations, and only Cx26Tag/Cx32 data is shown. In Figure 3, therefore, from left to right, the channels expressed contained less Cx26 and more Cx32. From top to bottom of each panel, the detergent

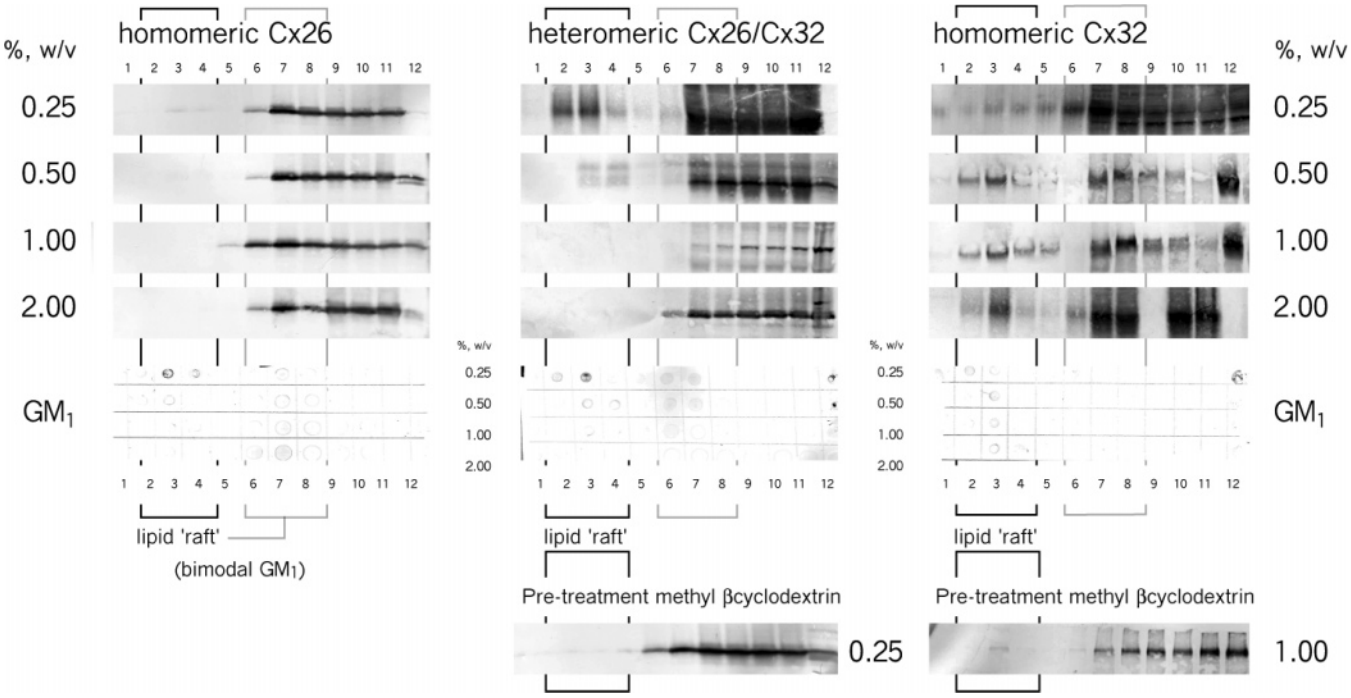

FIGURE 3: Cx32 channels are evident in TX100-insoluble raft fractions, less so with increasing Cx26 content. Confluent HeLa cell monolayers expressing homomeric Cx26, heteromeric Cx26/Cx32, or homomeric Cx32 channels (panels from left to right) were solubilized in 0.25%, 0.50%, 1.00%, or 2.00% TX100 (w/v, each row of Western blot from top to bottom). Ganglioside GM_1 is the raft marker, with the dot blots beneath each connexin Western blot showing the binding of CTB-HRP to an aliquot of the respective fractions. CD71 marked detergent-soluble nonraft fractions (see Figure 6). Western blotting shown in the figure was with monoclonal anti-HA to the CT $HA(HN)_6$ "tag", for comparative purposes between Cx26Tag in homomeric and heteromeric channels. Cell detergent lysates were fractionated though discontinuous sucrose gradients, and 12 fractions were collected. The flotation position of rafts was largely within fractions 3 and 4 in the gradient; of note, the distribution of GM_1 is bimodal (as observed by Radeva and Sharom (*26*)), with the second CT-HRP reactive peak in fractions 7 through 8. For depletion of cellular cholesterol, monolayers were preincubated with methyl β-cyclodextrin, as described in Materials and Methods, and after extensive washing were lysed in the indicated concentration of TX100. Data are representative of three independent experiments.

concentration doubles in successive rows. Dot blots showing the GM_1 raft marker in each of the recovered gradient fractions are shown below the anti-HA Western blots.

A small fraction of the homomeric Cx26 channels are found within GM_1-containing lipid raft fractions when prepared with 0.25% w/v TX100, a concentration well above the CMC of the detergent (Table 1). However, a greater fraction of Cx26 is in TX100-insoluble nonraft fractions. Above 0.25% w/v TX100, Cx26 is in raft fractions only when interacting with Cx32 in heteromeric channels (middle panel). Western blot with anti-HA of Cx26 from heteromeric Cx26Tag/Cx32 channels is shown for comparison with Cx26Tag in homomeric channels (left panel). Heteromeric channels show greater "stability" in TX100-insoluble raft membranes, present at up to 0.50% w/v TX100. In contrast, homomeric Cx32 channels (right panel) are raft associated in 2.00% w/v TX100, twice the concentration typically used for raft preparations. The presence of connexin channels in GM_1-inclusive rafts appears to correlate inversely with Cx26 content of the channel and with TX100 concentration. That is, Cx32 appears to stabilize the interaction of Cx26 with TX100-insoluble raft membranes.

NP40, from the same detergent family as TX100, has slightly different physicochemical character (Table 1). We determined the localization of the different connexin channels to GM_1-containing NP40-resistant raft fractions (Figure 4). As in Figure 3, Cx26 content in the channels decreases left to right as detergent concentration used increases from top to bottom. Connexin presence in these raft fractions resembles TX100-insoluble raft fractions with the difference that, at all detergent concentrations, there was complete exclusion of homomeric Cx26 channels from raft fractions. In addition, a greater fraction of Cx32 (as heteromeric or homomeric channels) is within detergent-insoluble nonraft rather than detergent-insoluble raft fractions.

Striking results were observed with Brij-58, from a detergent family different from NP40/TX100. Table 1 suggests that Brij-58 could be less effective than TX100/NP40 for membrane solubilization as its hydrophile−lipohile balance (HLB) reveals that a greater proportion of the chemical structure is "water-soluble" than "lipid-soluble". However, dot blotting with CTB-HRP suggested that isolation and enrichment of GM_1-containing raft membranes was, to some extent, better than with TX100/NP40. These lipid raft fractions contained the major fraction of homomeric Cx26 channels, whereas the major fraction of heteromeric Cx26/Cx32 channels and homomeric Cx32 channels was in nonraft fractions. That is, Cx32 appeared to *destabilize* the interaction of Cx26 with Brij-58-insoluble raft membranes. Recall that with NP40 or TX100 the opposite correlation was made. Methyl β-cyclodextrin pretreatment led to the dissolutions of raft microdomains by cholesterol depletion (32, *40*). Cx26-containing channels were then found within the heavier density gradient fractions. The flotation profile of homomeric Cx32 channels following cholesterol depletion was less markedly affected.

Finally, CD71 was used to confirm that the detergents used did not affect the gradient distribution of detergent-soluble

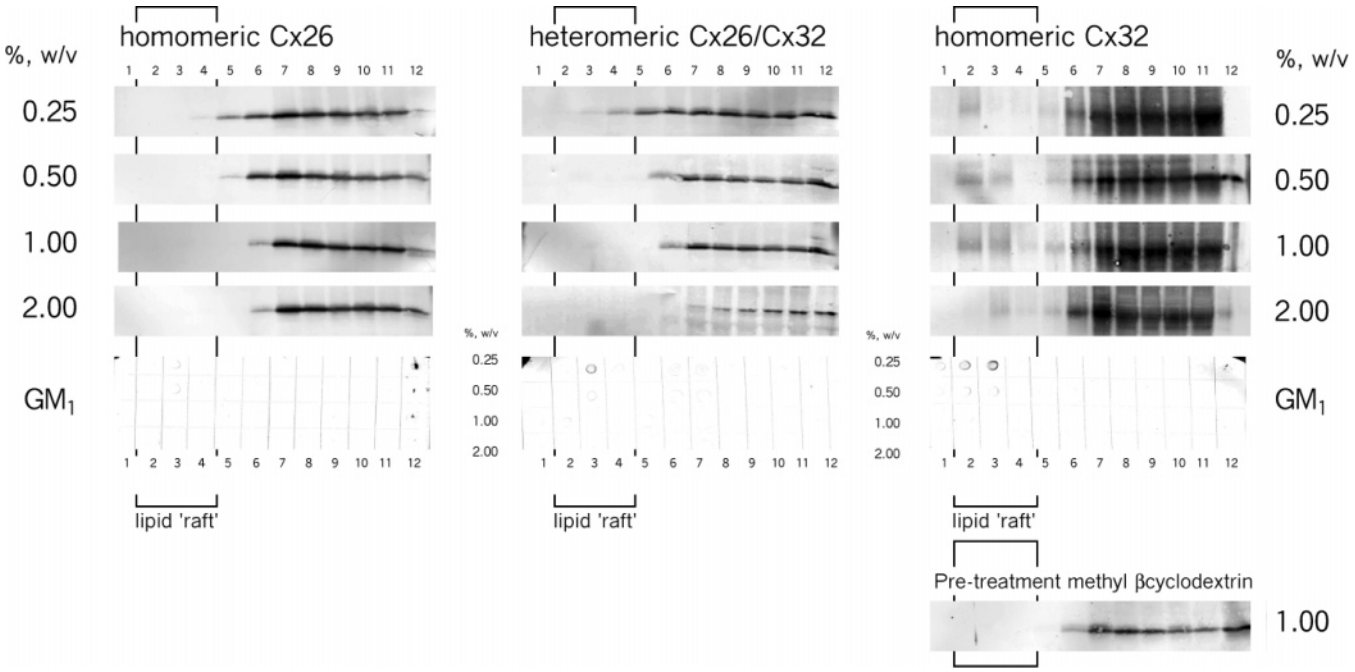

FIGURE 4: Cx32 channels in NP40-insoluble raft fractions, Cx26-containing channels excluded. Confluent HeLa cell monolayers, from left to right, expressing Cx26, Cx26/Cx32, or Cx32 channels were solubilized in 0.25%, 0.50%, 1.00%, or 2.00% (w/v) NP40, top to bottom. Refer to caption of Figure 3 for further details of Western blot. The GM_1 dot blots show that the rafts in these gradients are largely within fractions 2 and 3 of 12 collected. There was no GM_1 in gradient fractions with heavier density, as when TX100 was used. Cellular cholesterol was depleted with methyl β-cyclodextrin, and cells were lysed in the indicated concentration of NP40. Data shown are representative of three independent experiments.

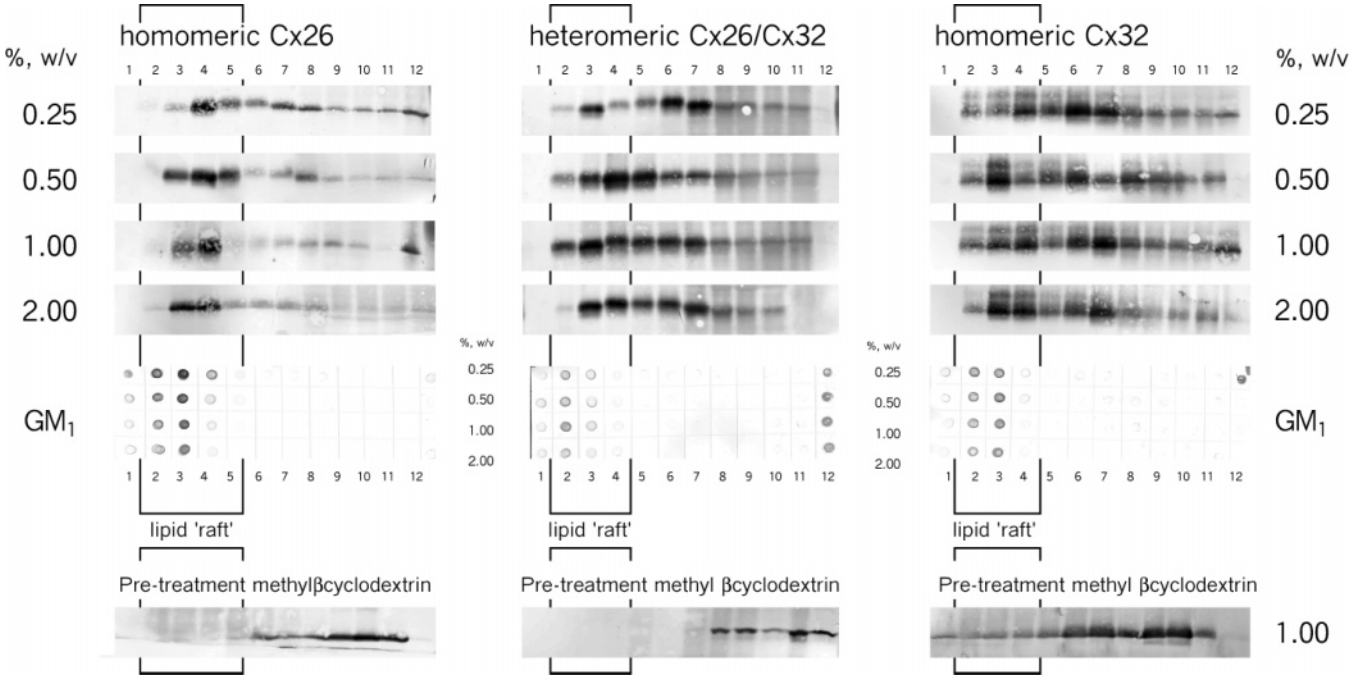

FIGURE 5: Brij-58-insoluble raft fractions enrich Cx26 channels; Cx32-containing channels partition between raft and nonraft membranes. Confluent HeLa cell monolayers (left to right) expressing Cx26, Cx26/Cx32, or Cx32 channels were solubilized in 0.25%, 0.50%, 1.00%, or 2.00% (w/v) Brij-58 (top to bottom). Refer to the caption of Figure 3 for further details of Western blot. GM_1 ganglioside dot blots with CTB-HRP mark the flotation of lipid rafts in these gradients, largely in fractions 2 and 3. Monolayers were preincubated with methyl β-cyclodextrin to deplete cholesterol, prior to lysis in the indicated concentration of Brij-58. Flotation profiles of Cx26-containing channels were markedly affected by cyclodextrin treatment, homomeric Cx32 channels less so. Data shown are representative of three independent experiments.

membrane protein (*26*, *38*). CD71 was completely solubilized by detergent, regardless of which detergent and detergent concentration was used (Figure 6). CD71 was always found in the higher or highest density nonraft gradient fractions, i.e., those collected from the bottom of the centrifugation tube.

Biochemical Analyses of Raft Fractions Prepared by Different Extraction Methods. The differences in connexin

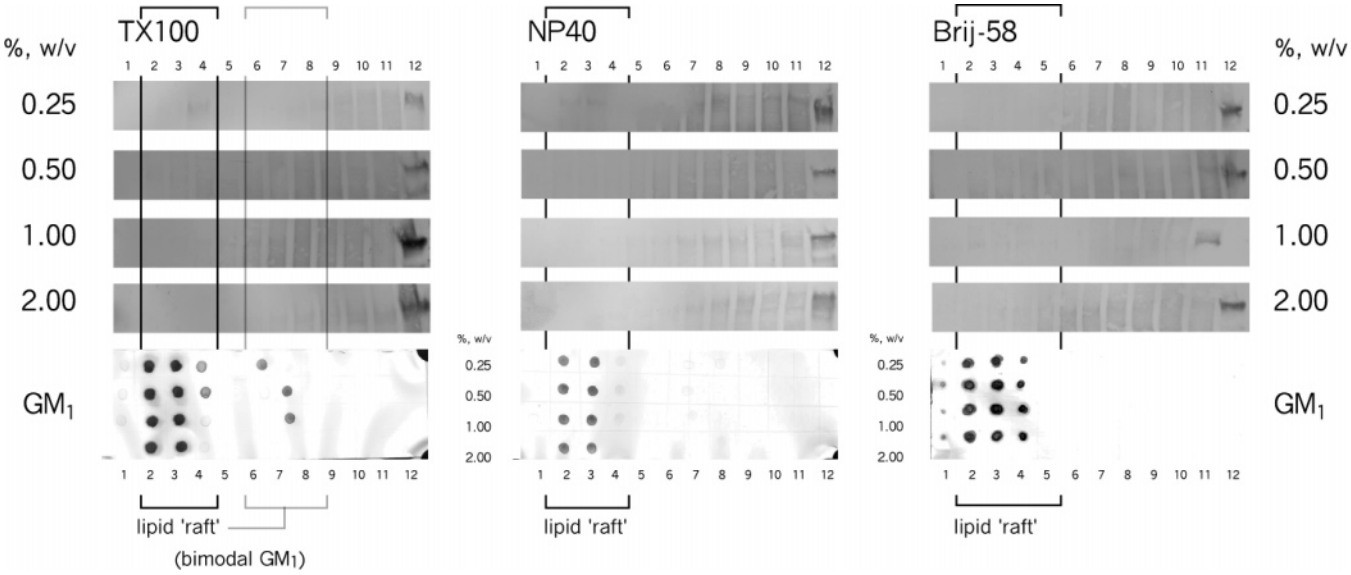

FIGURE 6: Distribution of raft-associated GM1 ganglioside and nonraft protein CD71 in fractions from the sucrose gradients. Confluent wild-type HeLa cell monolayers were solubilized in 0.25%, 0.50%, 1.00%, or 2.00% (w/v, top to bottom) TX100 (left), NP40 (center), or Brij-58 (right). Cell lysates were fractionated though discontinuous sucrose gradients, and 12 fractions were collected. GM_1 ganglioside dot blots with CTB-HRP mark the flotation of lipid rafts in these gradients, as used in Figures 2 through 5, although 5-fold more CTB-HRP (1/2000 dilution stock) was used to probe the blots (see Materials and Methods and Results). Western blotting was with a monoclonal antibody to CD71, the transferrin receptor, which is excluded from raft membranes in many cell types. GM_1- and CD71-containing gradient fractions do not overlap. Data shown are representative of three independent experiments.

content of raft fractions prepared by different methods (0.5 M Na_2CO_3 pH 11 or 0.25−2.00% w/v detergent pH 6.5, all 0−4 °C; Figures 2 through 6) suggested that the biochemical character of the rafts would likely be different as well (suggested also by refs *2*, *3*, *5*−*8*, *24*−*26*) (Figure 7).

Ganglioside GM_1 is a reliable end-point indicator for raft isolation (*2*, *3*, *5*−*8*, *24*−*26*, *32*, *34*). Enrichment of rafts in the upper sucrose gradient fractions was evident when comparing the density (Figure 7a−c) versus gradient distribution of GM_1 (Figure 7d−f) that was labeled prelysis on the HeLa cell surface by CTB-HRP. The density of the GM_1-containing raft fractions was slightly different depending on which extraction method was used. In the absence of detergent, rafts were in fractions 6 through 8 (of 12 recovered; density ∼1.114−1.151 g/cm^3). Rafts after lysis in Brij-58 were found in fractions 2 through 4 (∼1.058−1.089 g/cm^3). With NP40, rafts were largely in fractions 2 and 3 (∼1.056−1.086 g/cm^3), but in lower density fractions 3 and 4 using TX100 (∼1.076−1.100 g/cm^3).

Use of Brij-58 or alkaline carbonate rather than TX100 or NP40 also yielded raft fractions more enriched in GM_1 membranes, ∼9-fold and ∼6-fold greater respectively than with TX100/NP40. Visually, this was shown by the GM_1 dot blots of Figures 2 through 5; equivalent volume amounts of each fraction were loaded onto each GM_1 assay spot, and membranes were developed under the same conditions. This and Figure 7d−f are a more accurate representation of detergent-raft insolubility and recovery than Figure 6, when an excess of CTB-HRP was used for development and membranes were overexposed.

Of note, Figure 6 shows more clearly an artifact specific to TX100, that the GM_1 dot blot for TX100 is bimodal (Figure 7f; also observed by Radeva and Sharom (*26*)). The other detergents and alkaline carbonate enrich GM_1-containing membranes into the upper fractions of each gradient. The second TX100-insoluble GM_1 peak was in the higher density fractions 7 and 8 of the TX100 gradients (∼1.141−1.154 g/cm^3). Nevertheless, because the density is outside the range that corresponded to rafts prepared by other detergents, and because the related detergent NP40 does not produce this bimodal GM_1 distribution, we consider this an artifact specific to TX100.

All methods used "solubilized" a substantial amount of protein (Figure 7g−i). Protein content in raft fractions was an inverse function of the detergent concentration. However, raft fractions prepared by different means contained very different amounts of total protein. For instance, alkaline carbonate insoluble and Brij-58-insoluble raft fractions contained ∼5-fold and ∼3-fold more protein, respectively, than raft fractions prepared with TX100 and NP40, which had similar total protein content.

Phospholipid(s) (Figure 7j−l) and particularly cholesterol content (Figure 7m−o) were higher in all raft fractions compared with nonraft fractions. Notably, the total amount of lipids in alkaline carbonate insoluble and Brij-58-insoluble raft fractions was significantly greater (∼7-fold and ∼4-fold cholesterol, and ∼3-fold and ∼2-fold phospholipid(s), respectively) than after solubilization with TX100 or NP40, which had similar total lipid contents. The GM_1-containing fractions 7 and 8 of the TX100 gradients had very high protein content and therefore much lower lipid/protein ratio compared to fractions 3 and 4 (which are the TX100-insoluble membranes we refer to as rafts). However, these fractions did contain a minor cholesterol peak (Figure 7o).

This biochemical analysis shows that only the GM_1-containing upper gradient fractions (irrespective of extraction conditions used) contained membranes that are regarded as raft-derived, by accepted criteria (*4*, *5*).

Surface Colocalization of Nonjunctional Connexin Channels with Lipid Raft GM_1 Ganglioside. As raft fractions have been biochemically isolated containing different connexin channels, we investigated the native surface membrane

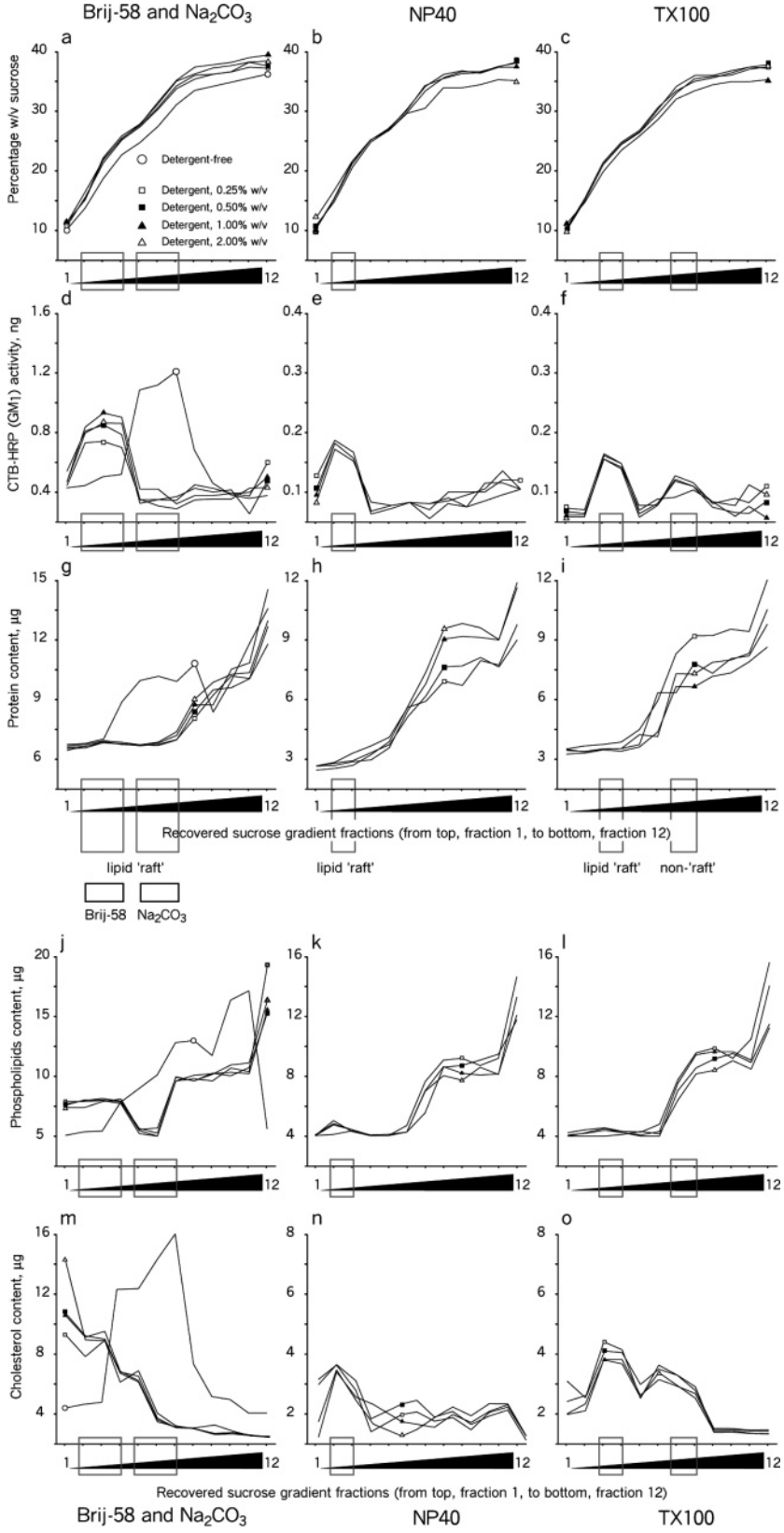

FIGURE 7: Biochemical analyses of raft and nonraft sucrose gradient fractions. HeLa cells expressed Cx26 (data shown in the figure), Cx32, or Cx26/Cx32 channels. Graphic represents one of three independent experiments for each cell line. Cells were extracted with nonionic detergents or alkaline carbonate. From left to right, Brij-58 pH 6.5 + Na_2CO_3 pH 11 (open circle) extracts, NP40 pH 6.5 extracts, and TX100 pH 6.5 extracts (detergent w/v concentrations: 0.25%, open square; 0.50%, closed square; 1.00%, open triangle; 2.00%, closed triangle). Separated gradient fractions, 12 in total where fraction 1 is the lightest (density; a−c), were assayed for the distribution of CTB-HRP prelabeled cell surface GM_1 ganglioside (d−f), and for total protein (g−i), total phospholipids (j−l), and cholesterol (m−o) content in each fraction. Please note that the *y*-abscissa scaling may differ. The protein content and GM_1 content (activity of CTB-HRP) is shown from a volume-adjusted aliquot of each recovered fraction. For cholesterol and phospholipid(s) analysis, content shown is for the entire fraction. The flotation positions of lipid raft fractions are boxed.

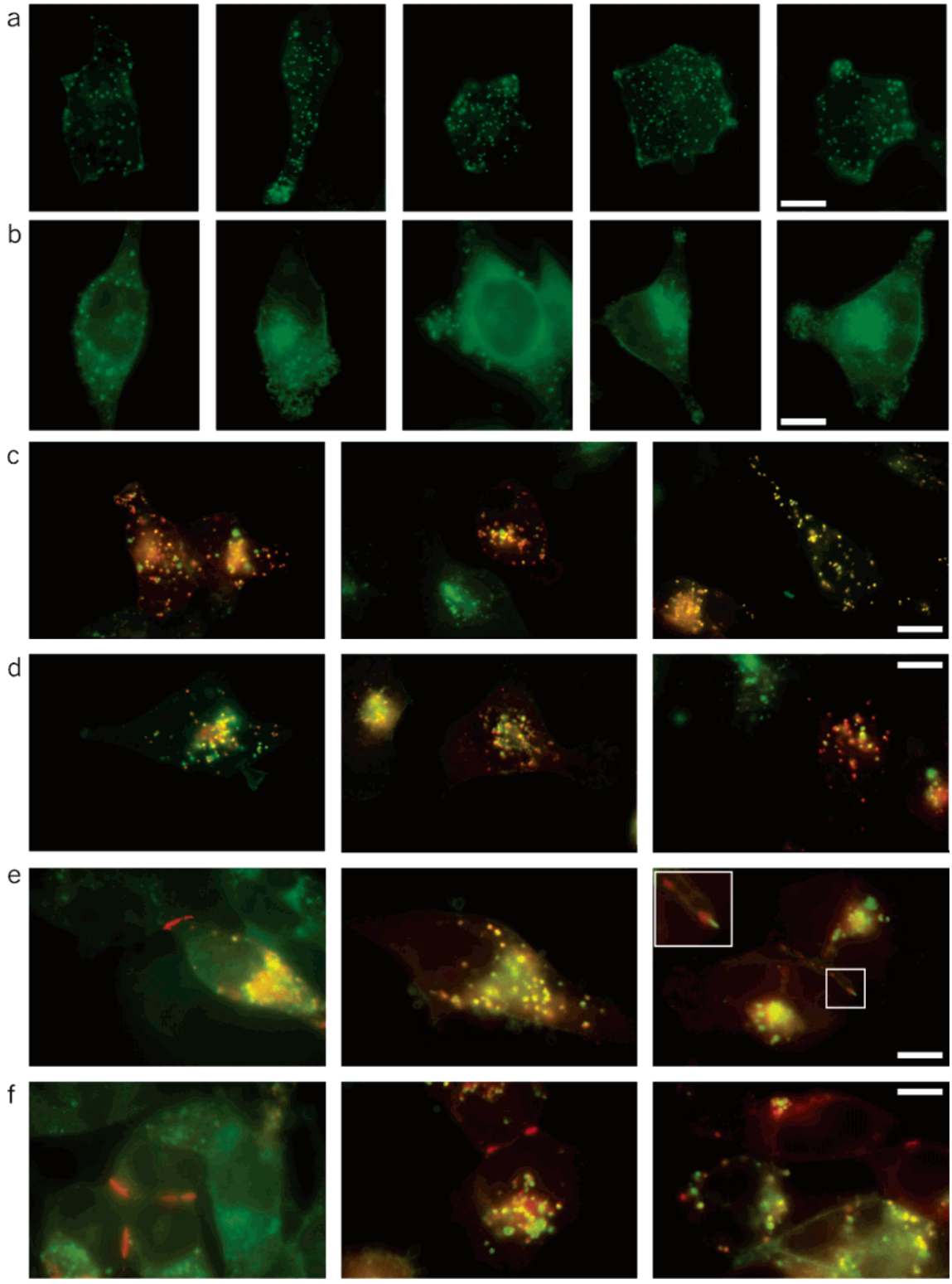

FIGURE 8: Cell surface labeling by CTB-FITC shows raft localization of Cx26 and/or Cx32 channels, but not connexin channels in gap junction plaques. Connexin-expressing HeLa cells were surface labeled with CTB-FITC at 4 °C (a, c, d) or 37 °C (leading to internalization of labeled membrane; b, e, f) prior to paraformaldehyde fixation and permeabilization for connexin staining. Cell lines were labeled using a specific monoclonal antibody to the hemagglutinin sequence of the CT $HA(HN)_6$ tag and Alexa594 labeled secondary. Merged focal images (c−f) present membrane CTX-FITC (green) and Cx26 (c, e) or Cx32 (d, f) channels (red). Extensive surface colocalization of Cx26 and/or Cx32 with CTB-FITC labeled membrane was observed (c, d). Staining was also coincident after CTB-FITC labeled membrane was internalized after staining at 37 °C (e, f). However, gap junctional membranes did not show coincident staining with CTB-FITC. Note in rightmost image of panels e (boxed, shown inset at higher magnification), an area of CTB-FITC labeled membrane associated en face with a region of gap junction cell−cell contact. Bar 5 μm.

associations between rafts and connexin channels (Figure 8). The cholera toxin receptor, ganglioside GM_1, is extensively used as a marker for raft domains (*2*, *3*, *5*−*8*, *24*−*26*, *32*, *34*). However at 37 °C, CTB is internalized via a caveolae/raft-dependent mechanism; surface labeling of GM_1 by CTB must be performed at 0−4 °C (*35*). When HeLa cells were

labeled with CTB-FITC at 4 °C, cell surface punctate labeling of GM_1 was observed (Figure 8a). At 37 °C, CTB-FITC labeled membrane was largely internalized; the supranuclear delivery suggesting Golgi localization, as previously shown (*35*) (Figure 8b).

Prominent, punctate immunofluorescence colocalization of homomeric (Figure 8c and 8d, for Cx26 and Cx32 respectively) connexin channels and CTB-FITC (4 °C) labeled membrane rafts was observed on the surface of HeLa cells. Not all Cx26 or Cx32 localized to raft membranes, and not all raft membrane was associated with connexin, as suggested by biochemical fractionation in Figures 3 through 5. Microscopy provided further indication that the association of connexin channels with rafts was not an artifact of detergent isolation.

Following CTB-FITC labeling at 37 °C, and internalization of labeled membrane, most nonjunctional connexin channels had also been internalized (however, we do not rule out that the supranuclear CTB-FITC localization overlapped connexin en route to the plasma membrane). Strikingly, gap junction plaques showed no labeling with CTB-FITC at 4 °C, and gap junction plaques were not internalized with CTB-FITC labeled raft membrane after 37 °C labeling (Figure 8e and 8f, for Cx26 and Cx32 respectively). In the rightmost image of Figure 8e, connexin immunostaining at junctional membrane is seen to abut but not overlap raft membrane staining by CTB-FITC.

When membrane preparations from homomeric Cx26 and Cx32 cell lines were solubilized with Brij-58 or TX100, at the same w/v concentrations used to prepare lipid rafts, both the GM_1-rich pellet and the supernatant contained connexin, confirming that there are raft-associated and nonraft connexin populations in plasma membrane (Figure 9). Given current thought that connexin channels accrete to junctional areas laterally from nonjunctional regions (see Discussion), these data raise the interesting possibility that different connexin channels make use of different rafts to move to and/or from the gap junction plaque.

Quantitative and Qualitative Differences in Lipid Character of Raft Fractions. Several lipid raft preparations from different cell types have recently been analyzed using various high-resolution methodologies to determine their lipid composition (*42*−*44*). All concur that many prior analyses do not have adequately described extraction protocols and that much of the data are nonquantitative. Using NP-HPLC and GC-FID, we carried out an analysis of the lipid species in different connexin-containing rafts. We hoped to provide direction for further work exploring connexin-specific lipid environments, an underexplored cell aspect of the biology of these channels (*45*).

Rafts were prepared with 1% w/v TX100 (from the homomeric Cx32 cell line; raft fractions 3 and 4), 1% w/v Brij-58 (from the homomeric Cx26 cell line), and 0.5 M Na_2CO_3 pH 11 (homomeric cell lines). We chose not to analyze NP40-insoluble raft fractions as Western blotting (Figure 4) suggested that these rafts were similar in connexin content to those prepared with TX100. Recall that raft fractions isolated in 1% w/v TX100 contain Cx32 but exclude Cx26 (Figure 3), and raft fractions prepared in 1% w/v Brij-58 enrich Cx26 (Figure 5).

NP-HPLC separations of recovered lipids showed that all raft preparations enriched cholesterol and phospholipids,

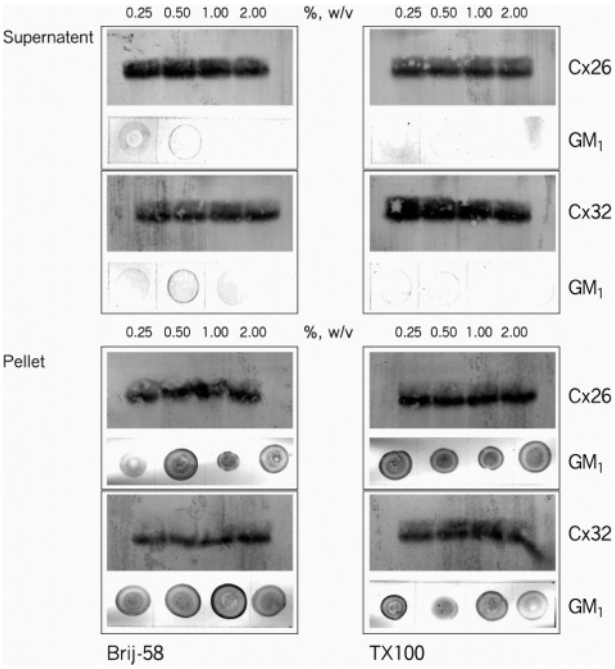

FIGURE 9: Detergent solubility of Cx26 and Cx32 in HeLa plasma membranes. Cell plasma membranes were prepared from HeLa cells using sucrose gradients, as described in Materials and Methods, then solubilized with Brij-58 or TX100 at concentrations used to prepare lipid rafts from whole cell lysates. Detergent-soluble (supernatant) and detergent-insoluble (pellet) fractions were blotted for GM_1 using CTB-HRP and for Cx26 or Cx32 using an anti-HA antibody to the CT epitope tag.

although there are quantitative and qualitative differences (Table 2: percentage w/w total lipid, Table 2a; mol %, Table 2b). The weight total lipid in Brij-58-insoluble raft fractions was ∼2-fold less than recovered in alkaline carbonate insoluble raft fractions. Total weight lipid in TX100-insoluble raft fractions was ∼5-fold less than in Brij-58-insoluble raft fractions (data not shown; "crude" analyses for Figure 7 had already shown this to be true).

Cholesterol (Chol) content was ∼3-fold higher in alkaline carbonate insoluble raft fractions than those insoluble in TX100 or Brij-58, likely due to this method preferentially enriching caveolin-1, a cholesterol-binding protein (*23*, *29*) (Figure 2). Percentage cholesterol content in Brij-58-insoluble raft fractions was similar to cholesterol content in TX100-insoluble raft fractions; however, TX100-insoluble raft fractions contained a higher percentage of triglycerides (TG) (∼3-fold higher) at the expense of phospholipid(s). The phospholipid composition of detergent-insoluble raft fractions, that contain either Cx32 (TX100) or Cx26 (Brij-58) channels, was similar except for negatively charged cardiolipin (CA) and phosphatidylglycerol (PG) phospholipids in Brij-58-insoluble raft fractions. Surprisingly, phosphatidylcholine (PC) was absent from raft fractions prepared with TX100, although PC membranes can be particularly soluble in this detergent (*43*).

GC-FID provided an analysis of the fatty acid composition (methylated esters; FAMEs) of the different phospholipids present in lipid raft fractions. The distribution by class of the (de)saturations indicated a high level of saturated FAMEs in raft fractions, whether they be prepared detergent-free or with detergents. When alkaline carbonate was used, more FAME species were present in raft fractions when compared

Table 2: Lipid Analysis of Raft Fractions[a]

	% w/w of total lipid					
extraction method (cell line)	TG	Chol	CA	PG	LPE	PC
TX100 (HeLa-Cx32)	36.70	20.96			42.34	
Brij-58 (HeLa-Cx26)	11.65	18.87	14.79	11.87	29.66	13.16
alkaline carbonate (HeLa-Cx32)	9.72	44.44				45.83
alkaline carbonate (HeLa-Cx26)	7.59	51.94			11.72	28.75

	mol % total lipid					
extraction method (cell line)	TG	Chol	CA	PG	LPE	PC
TX100 (HeLa-Cx32)	21.93	28.67			49.39	
Brij-58 (HeLa-Cx26)	7.71	28.59	6.79	8.73	38.33	9.8
alkaline carbonate (HeLa-Cx32)	5.95	62.39				31.64
alkaline carbonate (HeLa-Cx26)	4.04	66.51			12.17	17.26

	% w/w of total FAMEs							
extraction method (cell line)	$C_{16:0}$	$C_{18:0}$	$C_{18:1}$	$C_{18:2}$	$C_{18:3}$	$C_{20:1}$	$C_{20:2}$	$C_{20:4}$
TX100 (HeLa-Cx32)	69.69	18.18	6.07	6.06				
Brij-58 (HeLa-Cx26)	60.87	29.13						
alkaline carbonate (HeLa-Cx32)	20.98	23.04	22.22	4.73	10.28	2.11	4.3	12.34

[a] Details of lipid extraction, preparation for NP-HPLC and GC-FID, and assay conditions, including standards used, are given in Materials and Methods. Data shown is representative of raft′ fractions taken from three independent experiments.

with detergent-insoluble raft fractions, and a greater number of the FAMEs were desaturated with most containing more than one double bond. FAMEs in Brij-58-insoluble raft fractions were proportionally of longer chain length ($C_{18:0}$/$C_{16:0}$) than TX100-insoluble raft fractions. These latter raft fractions contained ~12% w/w shorter $C_{18:1}$ mono- and $C_{18:2}$ diunsaturated FAME species, which were absent from Brij-58-insoluble raft fractions. It is improbable that such unsaturated lipids are contaminants and not integral components of membrane rafts. A direct structural role for unsaturated lipids in rafts is possible since Chol forms condensed, ordered phases with monounsaturated phospholipids.

DISCUSSION

Cellular membranes were envisaged for many years as disordered uniform bilayers in which lipids moved freely and randomly by diffusion (*1*). A more recent view is that organized lipid raft microdomains exist within the fluid bilayer of plasma membrane (*4*, *5*), and localize a number of membrane proteins, including members of most channel families (*10*, *11*), while excluding others. The current model of raft lipid structure is such that the lipid composition confers resistance to solubilization by cold nonionic detergents or alkaline carbonate, which allows their recovery as insoluble membrane fractions by isopycnic centrifugation in sucrose density gradients (*5*−*7*).

This report provides dramatic examples of the targeting of different connexin isoforms (Cx26 and/or Cx32 channels; Figure 1) to lipid rafts prepared by different means (Figures 2 though 5). We found that subtle variations in biochemical methods used for raft preparation revealed profound and previously unsuspected differences in connexin channel distribution to membrane domains having different lipid composition (Figure 6, Figure 7, Table 2). Remarkably, immunocytochemistry showed that these connexin channels within raft fractions were not those channels within gap junction plaques but are likely unpaired hemichannels on the cell surface, perhaps en route to junctional membrane (Figure 8, Figure 9).

Such membrane organization is likely to have consequences for the physiology and cell biology of the connexin proteins involved. The homomeric and heteromeric Cx26 and/or Cx32 channels that were studied have demonstrated connexin-specific differences in their molecular permeability pathways and their modulation by cellular factors (*13*, *14*, *17*). Therefore, it is striking that these channels show dramatically distinct localizations among different types of rafts. It also suggests that subtle factors in the parts of each channel exposed to lipid can cause significant, previously unappreciated, differences in the specific lipid associations and/or the partitioning among membrane regions with different physicochemical properties.

Heterogeneity of Raft−*Connexin Interaction.* Lipid rafts are being viewed increasingly, not as homogeneous structures, but as a heterogeneous collection of microdomains with slightly different biophysical and biochemical characteristics, while nevertheless sharing common properties (*2*, *3*, *5*−*8*, *24*−*26*). This is illustrated by studies of polarized cells that show readily discernible separation of different membrane domains. For example, in T lymphocytes several proteins and the gangliosides GM_1 and GM_3, all of which associate with rafts, localize to different regions of the cells (*46*). These raft subsets play important physiological roles; liganding and signaling via the T-cell receptor takes place within distinct membrane raft domains (*38*, *47*). According to one recent model, different rafts may be distinct and nonadjacent (*48*). Alternatively, highly ordered rafts exist in proximity to semiordered domains that are more "soluble" (*5*, *48*) because of lipid heterogeneity. On mast cells, for instance, the FcγR1 receptor and its downstream signaling partner, LAT, are clustered in different, but adjacent, microdomains on the cell surface (*49*). These proteins also show differential detergent solubility.

Our results are consistent with either of these views. The presence of homomeric and heteromeric Cx26 and/or Cx32 channels in the lipid rafts of HeLa cells was determined first by insolubility experiments (Figures 3 through 5). Raft membrane fractions prepared with Triton X100 (TX100) or Nonidet P40 (NP40) contained Cx32 channels rather than Cx26-containing channels. In contrast, rafts prepared with Brij-58 enriched Cx26 channels over Cx32-containing channels. These data are also consistent with the work of Hand et al. (*36*), who used Brij-58 insolubility to enrich Cx26 channels from HeLa cells, and of Sikerwar and Malhotra (*50*), who used Brij-58 to enrich liver Cx26 and/or Cx32 channels, to the detriment of Cx32 content.

The structures of these detergents may account for their different actions. Brij-58 is characterized by a bulky C_{20} polyoxyethylene headgroup and saturated $C_{16:0}$ cetyl ether chain, and should preferentially partition into the loosely packed bulk lipid milieu rather than the ordered phase of the raft membrane (*51*, *52*). TX100/NP40 may have limited capability to distinguish raft domains from disordered bulk plasma membrane because of its structure (a phenol ring between the hydrophobic tail and the hydrophilic headgroup; *26*); the raft phase may be substantially solubilized by TX100, even at 0−4 °C (*6*). The density of GM_1 ganglioside rafts changed somewhat when different detergents were used (dot blots in Figures 2 through 6, Figure 7a−f). This might arise from the above-mentioned differential ability of TX100/NP40 and Brij-58 detergents to insert into the tight acyl-chain packing of raft lipids. As a result, various subpopulations of "insoluble" microdomains were isolated with the different detergents, each with specific connexin channel content.

In the present study, detergent-free fractionation by alkaline carbonate was also used to prepare rafts. Sucrose-density gradient sedimentation produced a heavy fraction and a light raft fraction (Figure 2). This method was designed especially to enrich caveolar rafts (*29*), a peculiar subset of raft membranes because it is the only subtype that can be distinguished morphologically (*23*). By this approach, both Cx26 and/or Cx32 channels were largely raft-associated. This supports previous work showing Cx26, Cx32 (and Cx43) to associate with caveolar rafts (*22*). However, in that study while caveolin-1 membrane colocalization with Cx43 was observed, there was no colocalization of both proteins at the gap junction; in fact, in the mammalian heart, caveolin-1 does not immunolocalize to the intercalated disk region where prominent Cx43 gap junctions are found. When we localized GM_1-containing raft and connexin on the surface of HeLa cells, we observed that gap junctions were not lipid rafts as such, but that nonjunctional connexin channels were localized to raft membranes (Figure 8). Detergent-free extraction and subsequent recovery of both raft and nonraft connexin in the same sucrose gradient fractions suggest that gap junctions share some biochemical or physicochemical properties of raft membranes. This low density of the plaque in sucrose gradients is perhaps due to associated lipids such as cholesterol, which are enriched in plaques (19, *45*).

Since the different nonionic detergents and alkaline carbonate method isolated rafts with slightly different biochemical character (Figure 7, Table 2), we entertained several possible interpretations. The first is that all rafts in vivo are identical, but different components (lipid and/or protein) are selectively "solubilized" by the different methods of preparation. We, and others, favor the second possibility, which is that in vivo rafts are heterogeneous with each raft subtype having a slightly different lipid and protein composition. In this case, the different methods of preparation select among different subpopulations (or overlapping subpopulations) of raft (*2*, *3*, *5*−*8*, *24*−*26*). A conservative interpretation is that different connexin channel forms and certain lipid domains share some physical−chemical relation, as they are differentially and selectively insoluble using the same techniques. That the differential solubilization takes place from the functional domains known as lipid rafts is particularly intriguing.

Biochemical Basis for Raft−Connexin Interaction. We investigated how these different raft fractions prepared by different means and containing different connexin channels differed in their lipid composition, or were similar. Methods for the isolation of connexin channels have been developed foremost to preserve the structural integrity of gap junction plaques, and few studies consider the associated lipids in their native states (*45*). Analyses of the lipid composition of hepatocyte gap junctions (Cx26 and/or Cx32 channels) by alkali or detergent extraction revealed substantial cholesterol enrichment relative to phospholipid (*19*), suggesting an important role for cholesterol in plaque assembly. Because cholesterol is also a key component of raft structure (*2*, *3*), a commonly used method for confirming raft association is by disruption of raft integrity or lipid content using cholesterol-modifying agents such as methyl β-cyclodextrin (*32*, *40*).

Our studies suggest that Cx26 and/or Cx32 channels are associated with heterogeneous cholesterol-based domains. We observed Cx26 only in raft fractions with high cholesterol content, i.e., those obtained in Brij-58 and alkaline carbonate, but not in cholesterol-poor raft membranes such as those insoluble in TX100/NP40 (Figure 7, Table 2). It is possible that Cx26 exists in membrane domains that have greater content of cholesterol than membrane domains containing Cx32. The effect of cholesterol depletion from cholesterol-rich Brij-58-insoluble membranes prior to raft isolation was more pronounced on homomeric Cx26 channels than homomeric Cx32 channels (Figure 5), reinforcing a strong association between Cx26 and cholesterol. That Cx26 and/or Cx32 gap junctions are also cholesterol-enriched, as suggested by (*19*), could also explain why they cofractionated with lipid rafts after detergent-free extraction and why methyl β-cyclodextrin treatment altered their buoyancy (Figure 2).

Another mechanism for the differential channel-raft association we observed may involve the differential thickness of the raft bilayers versus nonraft membrane. Saturated raft hydrocarbon chains are longer and straighter than saturated acyl chains in the surrounding phospholipid regions due to cholesterol intercalation. Therefore, bilayer thickness is slightly greater in raft domains (*2*, *3*). It is energetically favorable that the hydrophobic, membrane-spanning helices of these channel proteins match the thickness of the bilayer. Thus, minor differences in the length of the transmembrane domains of Cx26 and Cx32 proteins might increase or decrease their affinity for distinct lipid rafts. As well as cholesterol enrichments, we found a greater proportion of long length $C_{18:0}$ fatty acids in Cx26-inclusive rafts (Brij-58) than in Cx26-exclusive rafts (TX100), the latter also containing shortened desaturated species. It is premature to

conclude that this is evidence for connexin isoform-specific lipid associations, but we have shown that different connexin isoforms and certain lipid raft domains are selectively insoluble by the same means.

Functional Consequences for Raft−Connexin Interaction. One overall picture emerging is that rafts exert positive or negative control on signaling pathways (*5*, *8*, *9*). In their positive role, rafts containing different signaling proteins cluster or fuse upon agonist stimulation, resulting in the activation of signaling pathways. In their negative role, rafts spatially segregate interacting components to block nonspecific pathway activation, or through raft fusion directly suppress the activity of signaling proteins.

We have recently found by MALDI-MS that the CT terminal $C_{280}SAC_{283}$ sequence of Cx32 is palmitoylated (*53*, *62*), and others have found it prenylated (*63*). Saturated lipid modifications such as $C_{16:0}$ palmitoylation can improve raft affinity (*54*). Prenylation, a C_{15} or C_{20} desaturation, may aid in raft exclusion (*54*). For many proteins a small change of raft partitioning has been shown to initiate signaling cascades (*4*, *5*, *28*, *38*, *41*). The CT of Cx32 contains many of the channel regulatory elements. Different lipid modifications at the Cx32 CT may favor associations with raft domains of different lipid and protein compositions (in a raft continuum? *48*), which ensures tail proximity to signaling modulators, allowing dynamic regulation of channel function(s), and vice versa. Mutations $C_{280}G$ and $S_{281}X$ are implicated in CMTX (*55*, *56*). Given the nature of the mutation(s), it is tempting to attribute their pathology to raft mislocalization of the protein.

In addition, rafts themselves might have unique biophysical properties that directly affect connexin channel function. These parameters could include differences in lateral membrane pressure or surface charge compared with bulk membrane, fluidity and/or thickness as discussed. Perturbation of particular, surrounding lipid microenvironments could explain the activity and inactivity of many relatively nonspecific lipophiles on different connexin channels (*13*); much knowledge is phenomenological, and few studies have defined the correlative changes in channel subunit structure underlying these modulations. Lipid raft-connexin channel association might also function as a mechanism of regulation based on the proximity of different connexins to different lipid second messengers (*11*) rather than protein signaling modulators.

Our data suggest that rafts have consequences for Cx26 and/or Cx32 connexin channels with respect to junctional membrane targeting. Nonjunctional hemichannels exist on the surface of cells (*57*) (Figure 8), merging into the outside of existing gap junction plaques from which they are internalized (*58*). This dynamic process accurately regulates gap junction assembly and disassembly, but the means by which unpaired connexin hemichannels are (re)distributed to the gap junction remain largely unknown.

In a recently proposed model, the molecular address for raft-targeted proteins is the "lipid shell" (*48*). Theoretically, "shells" are smaller than rafts, acting as a local solvent for the single protein they harbor; larger raft structures form by shell fusion. Based on our results, we suggest the lipid raft (or shell) concept can accommodate the equilibrium between gap junction plaques and different unpaired hemichannels (single, or small clusters of) in nonjunctional membrane. Specifically, we suggest that rafts are key players in the dynamic redistribution and equilibrium between gap junction plaques and plasma membrane hemichannels. For example, in hepatocytes and transfected cells, homomeric and heteromeric Cx26 and/or Cx32 channels take different intracellular trafficking pathways to plasma membrane (*37*); there is no information on their relative movements to junctional plaques once within plasma membrane. Different lipid rafts may also be involved in this trafficking process, forming around different connexin channels in the intracellular pathway (*48*). Our data is also consistent with recent reports of Cx43 trafficking in osteoblasts that describe Cx43 first appearing on the plasma membrane in a raft compartment, where it does not form intercellular channels, requiring the tight junction protein ZO-1 for recruitment to the junctional membrane (*59*).

We have found that gap junctions are not rafts per se. Historically, the lack of effect of protein synthesis inhibitors on intercellular coupling supports the belief that unpaired connexin hemichannels exist in a form that permits rapid movement to the appositional junction region in the plasma membrane (*60*). Perhaps dynamic lipid raft membranes sequester and mobilize an available membrane "pool" of connexin channels.

REFERENCES

1. Singer, S. J. (2004) Some early history of membrane molecular biology, *Annu. Rev. Physiol. 66*, 1−27.
2. Edidin, M. (2003) The state of lipid rafts: from model membranes to cells, *Annu. Rev. Biophys. Biomol. Struct. 32*, 257−83.
3. de Almeida, R. F., Fedorov, A., and Prieto, M. (2003) Sphingomyelin/phosphatidylcholine/cholesterol phase diagram: boundaries and composition of lipid rafts, *Biophys. J. 85*, 2406−16.
4. Simons, K., and Ikonen, E. (1997) Functional rafts in cell membranes, *Nature 387*, 569−72.
5. Simons, K., and Vaz, W. L. (2004) Model systems, lipid rafts, and cell membranes, *Annu. Rev. Biophys. Biomol. Struct. 33*, 269−95.
6. Shogomori, H., and Brown, D. A. (2003) Use of detergents to study membrane rafts: the good, the bad, and the ugly, *Biol. Chem. 384*, 1259−63.
7. Luria, A., Vegelyte-Avery, V., Stith, B., Tsvetkova, N. M., Wolkers, W. F., Crowe, J. H., Tablin, F., and Nuccitelli, R. (2002) Detergent-free domain isolated from Xenopus egg plasma membrane with properties similar to those of detergent-resistant membranes, *Biochemistry 41*, 13189−97.
8. Draber, P., and Draberova, L. (2002) Lipid rafts in mast cell signaling, *Mol. Immunol. 38*, 1247−52.
9. Pike, L. J. (2003) Lipid rafts: bringing order to chaos, *J. Lipid Res. 44*, 655−67.
10. O'Connell, K. M., Martens, J. R., and Tamkun, M. M. (2004) Localization of ion channels to lipid Raft domains within the cardiovascular system, *Trends Cardiovasc. Med. 14*, 37−42.
11. Tillman, T. S., and Cascio, M. (2003) Effects of membrane lipids on ion channel structure and function, *Cell Biochem. Biophys. 38*, 161−90.
12. Willecke, K., Eiberger, J., Degen, J., Eckardt, D., Romualdi, A., Guldenagel, M., Deutsch, U., and Sohl, G. (2002) Structural and functional diversity of connexin genes in the mouse and human genome, *Biol. Chem. 383*, 725−37.
13. Harris, A. L. (2001) Emerging issues of connexin channels: biophysics fills the gap, *Q. Rev. Biophys. 34*, 325−472.
14. Locke, D., Stein, T., Davies, C., Morris, J., Harris, A. L., Evans, W. H., Monaghan, P., and Gusterson, B. (2004) Altered permeability and modulatory character of connexin channels during mammary gland development, *Exp. Cell Res. 298*, 643−60.
15. Bedner, P., Niessen, H., Odermatt, B., Willecke, K., and Harz, H. (2003) A method to determine the relative cAMP permeability of connexin channels, *Exp. Cell Res. 291*, 25−35.

16. Goldberg, G. S., Moreno, A. P., and Lampe, P. D. (2002) Gap junctions between cells expressing connexin 43 or 32 show inverse permselectivity to adenosine and ATP, *J. Biol. Chem. 277*, 36725−30.
17. Bevans, C. G., Kordel, M., Rhee, S. K., and Harris, A. L. (1998) Isoform composition of connexin channels determines selectivity among second messengers and uncharged molecules, *J. Biol. Chem. 273*, 2808−16.
18. Veenstra, R. D. (1996) Size and selectivity of gap junction channels formed from different connexins, *J. Bioenerg. Biomembr. 28*, 327−37.
19. Henderson, D., Eibl, H., and Weber, K. (1979) Structure and biochemistry of mouse hepatic gap junctions, *J. Mol. Biol. 132*, 193−218.
20. Alcala, J., Katar, M., and Maisel, H. (1982) Lipid composition of chick lens fiber cell gap junctions, *Curr. Eye Res. 2*, 569−78.
21. Lin, D., Zhou, J., Zelenka, P. S., and Takemoto, D. J. (2003) Protein kinase Cgamma regulation of gap junction activity through caveolin-1-containing lipid rafts, *Invest. Ophthalmol. Visual Sci. 44*, 5259−68.
22. Schubert, A. L., Schubert, W., Spray, D. C., and Lisanti, M. P. (2002) Connexin family members target to lipid raft domains and interact with caveolin-1, *Biochemistry 41*, 5754−64.
23. Bathori, G., Cervenak, L., and Karadi, I. (2004) Caveolae−an alternative endocytotic pathway for targeted drug delivery, *Crit. Rev. Ther. Drug Carrier Syst. 21*, 67−95.
24. Schuck, S., Honsho, M., Ekroos, K., Shevchenko, A., and Simons, K. (2003) Resistance of cell membranes to different detergents, *Proc. Natl. Acad. Sci. U.S.A 100*, 5795−800.
25. Brown, D. A., and London, E. (1998) Functions of lipid rafts in biological membranes, *Annu. Rev. Cell Dev. Biol. 14*, 111−36.
26. Radeva, G., and Sharom, F. J. (2004) Isolation and characterization of lipid rafts with different properties from RBL-2H3 (rat basophilic leukaemia) cells, *Biochem. J. 380*, 219−30.
27. Koreen, I. V., Elsayed, W. A., Liu, Y. J., and Harris, A. L. (2004) Tetracycline-regulated expression enables purification and functional analysis of recombinant connexin channels from mammalian cells, *Biochem. J. 383*, 111−9.
28. Locke, D., Chen, H., Liu, Y., Liu, C., and Kahn, M. L. (2002) Lipid rafts orchestrate signaling by the platelet receptor glycoprotein VI, *J. Biol. Chem. 277*, 18801−9.
29. Song, K. S., Li, S., Okamoto, T., Quilliam, L. A., Sargiacomo, M., and Lisanti, M. P. (1996) Co-purification and direct interaction of Ras with caveolin, an integral membrane protein of caveolae microdomains. Detergent-free purification of caveolae microdomains, *J. Biol. Chem. 271*, 9690−7.
30. Bligh, E. G., and Dyer, W. J. (1959) A rapid method of total lipid extraction and purification, *Can. J. Biochem. Physiol. 37*, 911−7.
31. Zlatkis, A., Zak, B., and Boyle, A. J. (1953) new method for the direct determination of serum cholesterol, *J. Lab. Clin. Med. 41*, 486−92.
32. Giocondi, M. C., Milhiet, P. E., Dosset, P., and Le Grimellec, C. (2004) Use of cyclodextrin for AFM monitoring of model raft formation, *Biophys. J. 86*, 861−9.
33. Kyaw, A., Maung, U. K., and Toe, T. (1985) Determination of inorganic phosphate with molybdate and Triton X-100 without reduction, *Anal. Biochem. 145*, 230−4.
34. Blank, N., Gabler, C., Schiller, M., Kriegel, M., Kalden, J. R., and Lorenz, H. M. (2002) A fast, simple and sensitive method for the detection and quantification of detergent-resistant membranes, *J. Immunol. Methods 271*, 25−35.
35. Pang, H., Le, P. U., and Nabi, I. R. (2004) Ganglioside GM1 levels are a determinant of the extent of caveolae/raft-dependent endocytosis of cholera toxin to the Golgi apparatus, *J. Cell Sci. 117*, 1421−30.
36. Hand, G. M. (2002) Isolation and characterization of gap junctions from tissue culture cells, *J. Mol. Biol. 315*, 587−600.
37. Evans, W. H., and Martin, P. E. (2002) Gap junctions: structure and function (Review), *Mol. Membr. Biol. 19*, 121−36.
38. Giurisato, E., McIntosh, D. P., Tassi, M., Gamberucci, A., and Benedetti, A. (2003) T cell receptor can be recruited to a subset of plasma membrane rafts, independently of cell signaling and attendantly to raft clustering, *J. Biol. Chem. 278*, 6771−8.
39. Razani, B., Rubin, C. S., and Lisanti, M. P. (1999) Regulation of cAMP-mediated signal transduction via interaction of caveolins with the catalytic subunit of protein kinase A, *J. Biol. Chem. 274*, 26353−60.
40. Lawrence, J. C., Saslowsky, D. E., Edwardson, J. M., and Henderson, R. M. (2003) Real-time analysis of the effects of cholesterol on lipid raft behavior using atomic force microscopy, *Biophys. J. 84*, 1827−32.
41. Holowka, D., and Baird, B. (2001) Fc(epsilon)RI as a paradigm for a lipid raft-dependent receptor in hematopoietic cells, *Semin. Immunol. 13*, 99−105.
42. Koumanov, K. S., Tessier, C., Momchilova, A. B., Rainteau, D., Wolf, C., and Quinn, P. J. (2005) Comparative lipid analysis and structure of detergent-resistant membrane raft fractions isolated from human and ruminant erythrocytes, *Arch. Biochem. Biophys. 434*, 150−8.
43. Baron, C. B., and Coburn, R. F. (2004) Smooth muscle raft-like membranes, *J. Lipid. Res. 45*, 41−53.
44. Rivas, M. G., and Gennaro, A. M. (2003) Detergent resistant domains in erythrocyte membranes survive after cell cholesterol depletion: an EPR spin label study, *Chem. Phys. Lipids 122*, 165−9.
45. Malewicz, B., Kumar, V. V., Johnson, R. G., and Baumann, W. J. (1990) Lipids in gap junction assembly and function, *Lipids 25*, 419−27.
46. Spiegel, S., Kassis, S., Wilchek, M., and Fishman, P. H. (1984) Direct visualization of redistribution and capping of fluorescent gangliosides on lymphocytes, *J. Cell Biol. 99*, 1575−81.
47. Drevot, P., Langlet, C., Guo, X. J., Bernard, A. M., Colard, O., Chauvin, J. P., Lasserre, R., and He, H. T. (2002) TCR signal initiation machinery is pre-assembled and activated in a subset of membrane rafts, *EMBO J. 21*, 1899−908.
48. Helms, J. B., and Zurzolo, C. (2004) Lipids as targeting signals: lipid rafts and intracellular trafficking, *Traffic 5*, 247−54.
49. Oliver, J. M., Pfeiffer, J. R., Surviladze, Z., Steinberg, S. L., Leiderman, K., Sanders, M. L., Wofsy, C., Zhang, J., Fan, H., Andrews, N., Bunge, S., Boyle, T. J., Kotula, P., and Wilson, B. S. (2004) Membrane receptor mapping: the membrane topography of Fc(epsilon)RI signaling, *Subcell. Biochem. 37*, 3−34.
50. Sikerwar, S. S., and Malhotra, S. K. (1983) A structural characterization of gap junctions isolated from mouse liver, *Cell Biol. Int. Rep. 7*, 897−903.
51. Luche, S., Santoni, V., and Rabilloud, T. (2003) valuation of nonionic and zwitterionic detergents as membrane protein solubilizers in two-dimensional electrophoresis, *Proteomics 3*, 249−53.
52. Johansson, F., Olbe, M., Sommarin, M., and Larsson, C. (1995) Brij 58, a polyoxyethylene acyl ether, creates membrane vesicles of uniform sidedness. A new tool to obtain inside-out (cytoplasmic side-out) plasma membrane vesicles, *Plant J. 7*, 165−73.
53. Locke, D., Koreen, I. V., Hertzberg, E., and Harris, A. L. (2005) Isoelectric focusing of intact connexin hemichannels, *Biophys. J. 88*, 267a.
54. Resh, M. D. (2004) Membrane targeting of lipid modified signal transduction proteins, *Subcell. Biochem. 37*, 217−32.
55. Castro, C., Gomez-Hernandez, J. M., Silander, K., and Barrio, L. C. (1999) Altered formation of hemichannels and gap junction channels caused by C-terminal connexin-32 mutations, *J. Neurosci. 19*, 3752−60.
56. Yum, S. W., Kleopa, K. A., Shumas, S., and Scherer, S. S. (2002) Diverse trafficking abnormalities of connexin32 mutants causing CMTX, *Neurobiol. Dis. 11*, 43−52.
57. Goodenough, D. A., and Paul, D. L. (2003) Beyond the gap: functions of unpaired connexon channels, *Nat. Rev. Mol. Cell Biol. 4*, 285−94.
58. Gaietta, G., Deerinck, T. J., Adams, S. R., Bouwer, J., Tour, O., Laird, D. W., Sosinsky, G. E., Tsien, R. Y., and Ellisman, M. H. (2002) Multicolor and electron microscopic imaging of connexin trafficking, *Science 296*, 503−7.
59. Laing, J. G., Chou, B. C., and Steinberg, T. H. (2005) ZO-1 alters the plasma membrane localization and function of Cx43 in osteoblastic cells, *J. Cell Sci. 118*, 2167−76.
60. Chow, I., and Poo, M. M. (1984) Formation of electrical coupling between embryonic Xenopus muscle cells in culture, *J. Physiol. 346*, 181−94.
61. Helenius, A., McCaslin, D. R., Fries, E., and Tanford, C. (1979) Properties of detergents, *Methods Enzymol. 56*, 734−49.
62. Koreen, I. V. Ph.D. Dissertation, University of Medicine and Dentistry of New Jersey, Newark, New Jersey, 2004.
63. Huang, Y., Sirkowski, E. E., Stickney, J. T., and Scherer, S. S. (2005) Prenylation-defective human connexin32 mutants are normally localized and function equivalently to wild-type connexin32 in myelinating Schwann cells. *J. Neurosci. 25*, 7111−20.

BI050495A